

# Synthesis, X-ray powder diffraction and DFT-d studies of indole-based compounds

ElSayed M. Shalaby\*, Aladdin M. Srour, Siva S. Panda, Riham F. George, Andrew N. Fitch and Adel S. Girgis\*

**\*Corresponding authors: ElSayed M. Shalaby**, X-Ray Crystallography Lab., Physics Division, National Research Centre, Dokki, Giza 12622, Egypt, E-mail: sayedshalaby@gmail.com; **Adel S. Girgis**, Pesticide Chemistry Department, National Research Centre, Dokki, Giza 12622, Egypt, E-mail: girgisas10@yahoo.com

**Aladdin M. Srour**: Therapeutical Chemistry Department, National Research Centre, Dokki, Giza 12622, Egypt

**Siva S. Panda**: Department of Chemistry & Physics, Augusta University, Augusta, GA 30912, USA

**Riham F. George**: Pharmaceutical Chemistry Department, Faculty of Pharmacy, Cairo University, Cairo, Egypt

**Andrew N. Fitch**: European Synchrotron Radiation Facility, CS40220, 38043 Grenoble Cedex 9, France

## Supplementary material

### Table titles

**Table 1.** Selected intramolecular experimental (X-ray) and computational optimized geometrical parameters (bond lengths, Å) of compounds **4a–d**.

**Table S2.** Selected intramolecular experimental (X-ray) and computational optimized geometrical parameters (bond angles, °) of compounds **4a–d**.

**Table S3:** Hydrogen-bond geometry (Å, °) of compound **4a**.

**Table S4:** Hydrogen-bond geometry (Å, °) of compound **4b**.

**Table S5:** Hydrogen-bond geometry (Å, °) of compound **4c**.

**Table S6:** Hydrogen-bond geometry (Å, °) of compound **4d**.

## Figure captions

**Fig. S1.** IR spectrum of compound **4a** (KBr pellet).

**Fig. S2.**  $^1\text{H}$ -NMR spectrum of compound **4a** in  $\text{CDCl}_3$ .

**Fig. S3.**  $^{13}\text{C}$ -NMR spectrum of compound **4a** in  $\text{CDCl}_3$ .

**Fig. S4.** IR spectrum of compound **4b** (KBr pellet).

**Fig. S5.**  $^1\text{H}$ -NMR spectrum of compound **4b** in  $\text{CDCl}_3$ .

**Fig. S6.**  $^{13}\text{C}$ -NMR spectrum of compound **4b** in  $\text{CDCl}_3$ .

**Fig. S7.** IR spectrum of compound **4c** (KBr pellet).

**Fig. S8.**  $^1\text{H}$ -NMR spectrum of compound **4c** in  $\text{CDCl}_3$ .

**Fig. S9.**  $^{13}\text{C}$ -NMR spectrum of compound **4c** in  $\text{CDCl}_3$ .

**Fig. S10.** IR spectrum of compound **4d** (KBr pellet).

**Fig. S11.**  $^1\text{H}$ -NMR spectrum of compound **4d** in  $\text{CDCl}_3$ .

**Fig. S12.**  $^{13}\text{C}$ -NMR spectrum of compound **4d** in  $\text{CDCl}_3$ .

**Fig. S13.** A projection of the optimized structure of compound **4a** by DFT/B3LYP method with 6-31G(d,p) basis set.

**Fig. S14.** A projection of the optimized structure of compound **4b** by DFT/B3LYP method with 6-31G(d,p) basis set.

**Fig. S15.** A projection of the optimized structure of compound **4c** by DFT/B3LYP method with 6-31G(d,p) basis set.

**Fig. S16.** A projection of the optimized structure of compound **4d** by DFT/B3LYP method with 6-31G(d,p) basis set.

**Fig. S17.** Effect of compound **4a** on contracture induced by histamine in isolated guinea pig tracheal rings.

**Fig. S18.** Effect of compound **4b** on contracture induced by histamine in isolated guinea pig tracheal rings.

**Fig. S19.** Effect of compound **4c** on contracture induced by histamine in isolated guinea pig tracheal rings.

**Fig. S20.** Effect of compound **4d** on contracture induced by histamine in isolated guinea pig tracheal rings.

**Fig. S21.** Effect of theophylline on contracture induced by histamine in isolated guinea pig tracheal rings.

**Fig. S22.** Overlay view of compound **4a**, red (X-ray structure), green (free state DFT), yellow (DFT validation).

**Fig. S23.** Overlay view of compound **4b**, red (X-ray structure), green (free state DFT), yellow (DFT validation).

**Fig. S24.** Overlay view of compound **4c**, red (X-ray structure), green (free state DFT), yellow (DFT validation).

**Fig. S25.** Overlay view of compound **4d**, red (X-ray structure), green (free state DFT), yellow (DFT validation).

**Fig. S26.** The molecular structure of compound **4a** showing the atom-labeling scheme and the refined torsion angles (green arrows).

**Fig. S27.** The molecular structure of compound **4b** showing the atom-labeling scheme and the refined torsion angles (green arrows).

**Fig. S28.** The molecular structure of compound **4c** showing the atom-labeling scheme and the refined torsion angles (green arrows).

**Fig. S29.** Crystal packings in **4a**. Dashed lines denote intermolecular interactions.

**Fig. S30.** Crystal packings in **4b**. Dashed lines denote intermolecular interactions.

**Fig. S31.** Crystal packings in **4c**. Dashed lines denote intermolecular interactions.

**Table 1.** Selected intramolecular experimental (X-ray) and computational optimized geometrical parameters (bond lengths, Å) of compounds **4a–d**.

Geometric parameters	Compd. <b>4a</b>		Compd. <b>4b</b>		Compd. <b>4c</b>		Compd. <b>4d</b>	
	Exp. X-ray data	DFT-d	Exp. X-ray data	DFT-d	Exp. X-ray data	DFT-d	Exp. X-ray data	DFT-d
O1—C1	1.4342	1.4408	1.4393	1.44	1.4382	1.4409	1.4472	1.4408
O1—C2	1.3391	1.3455	1.3437	1.3473	1.3474	1.349	1.3757	1.3507
N1—C2	1.3116	1.3249	1.3108	1.3254	1.3219	1.3225	1.29	1.3216
C2—C3	1.4136	1.4185	1.4124	1.4197	1.4035	1.4184	1.4136	1.4178
C3—C4	1.4193	1.4094	1.4274	1.4124	1.4513	1.411	1.411	1.4078
N2—C4	1.1574	1.1842	1.1457	1.1847	1.1392	1.1851	1.1631	1.1853
C3—C5	1.4084	1.4153	1.396	1.4153	1.3802	1.4176	1.3889	1.4187
C5—C6	1.4549	1.4546	1.4686	1.4556	1.4648	1.4561	1.4293	1.4519
C6—C7	1.3759	1.3879	1.3592	1.3879	1.3493	1.3868	1.3577	1.3897
N3—C7	1.3624	1.3721	1.3526	1.3718	1.3745	1.3702	1.3427	1.3664
N3—C22	1.4525	1.4648	1.4599	1.4516	1.4692	1.459	1.4898	1.4598
N3—C8	1.3789	1.3885	1.3701	1.3877	1.3838	1.3876	1.373	1.3865
C8—C9	1.3913	1.3969	1.4004	1.3965	1.4032	1.3952	1.377	1.3938
C9—C10	1.3821	1.3904	1.3759	1.3898	1.3593	1.3896	1.3784	1.3877
C10—C11	1.4011	1.4058	1.3854	1.4062	1.3985	1.4062	1.4138	1.4053

C11—C12	1.3826	1.3883	1.3817	1.3891	1.3779	1.3888	1.3775	1.3899
C12—C13	1.3989	1.4041	1.394	1.4046	1.3913	1.4035	1.399	1.4057
C8—C13	1.4115	1.4214	1.4213	1.4229	1.4038	1.4236	1.4214	1.4237
C6—C13	1.4449	1.4436	1.4375	1.4457	1.4426	1.4451	1.4325	1.448
C5—C14	1.398	1.4025	1.3901	1.4035	1.4095	1.4022	1.3914	1.4012
C14—C15	1.3839	1.3941	1.3874	1.3942	1.382	1.3962	1.3773	1.3952
N1—C15	1.3437	1.3579	1.3603	1.3591	1.3524	1.3572	1.3727	1.3583
C15—C16	1.478	1.475	1.4702	1.4769	1.4726	1.4736	1.4721	1.4695
C16—C17	1.3965	1.4025	1.3952	1.4037	1.387	1.4053	1.395	1.406
C17—C18	1.3854	1.3865	1.3812	1.3875	1.3855	1.3861	1.3703	1.3808
C18—C19	1.3888	1.394	1.3746	1.3951	1.382	1.4018	1.3805	1.4021
C19—C20	1.3884	1.3939	1.372	1.3951	1.3682	1.3998	1.3807	1.4
C20—C21	1.3851	1.3916	1.3937	1.3884	1.3771	1.3891	1.3782	1.3884
C16—C21	1.3986	1.4031	1.3867	1.4038	1.3776	1.4009	1.3858	1.4
O2—C19							1.3748	1.3631
O2—C24							1.4197	1.4332
C22—C23	1.524	1.5161			1.4749	1.5236	1.5264	1.5243
C19—C24					1.5288	1.4984		
Cl1—C19			1.7461	1.7273				
RMSE	0.009067929		0.015306		0.021757957		0.017200336	

Maximum difference	0.0268	0.039	0.0487	0.032
--------------------	--------	-------	--------	-------

**Table S2.** Selected intramolecular experimental (X-ray) and computational optimized geometrical parameters (bond angles, °) of compounds **4a–d**.

Geometric parameters	Compd. <b>4a</b>		Compd. <b>4b</b>		Compd. <b>4c</b>		Compd. <b>4d</b>	
	Exp. X-ray data	DFT-d	Exp. X-ray data	DFT-d	Exp. X-ray data	DFT-d	Exp. X-ray data	DFT-d
C1—O1—C2	117.63	118.25	118.5	118.22	117.71	116.83	116.27	117.26
C7—N3—C22	125.98	127.31	126.08	125.6	125.58	125	125.27	125.29
O1—C2—C3	116.48	116.19	114.52	115.82	115.54	116.69	112.7	115.99
C2—C3—C5	117.85	117.76	117.47	117.86	118.53	117.78	119.73	117.89
C3—C5—C6	124.23	122.78	123.03	122.96	123.86	122.34	124.44	123.02
C5—C6—C7	127.86	127.43	126.91	126.69	125.59	125.9	128.24	126.22
N3—C7—C6	110.64	110.43	111.42	110.55	111.33	110.7	111.13	110.81
C9—C8—C13	122.5	122.6	122.11	122.85	123.07	122.81	124.33	122.96
C10—C11—C12	121.18	121.16	120.48	121.24	121.14	121.26	120.57	121.26
C6—C13—C12	134.99	134.56	134.84	134.71	135.06	134.74	138.78	135.22
N1—C15—C14	121.24	121.05	121.42	121.16	121.88	121.06	121.15	120.96
C15—C16—C17	119.64	119.04	120.16	119.49	119.73	119.42	120.8	119.55
C16—C17—C18	120.65	121.03	122.16	121.61	121.05	121.26	121.9	121.66
C16—C21—C20	120.82	120.67	121.75	121.32	121.88	120.93	123.59	122.01
C2—N1—C15	119	118.74	117.28	118.6	117.16	118.89	115.82	118.5

C8—N3—C22	125.11	124.04	125.09	125.53	126.53	126.14	126.27	125.93
N1—C2—C3	123.77	123.91	125.27	124.06	124.78	123.99	125.85	124.35
C4—C3—C5	122	123.45	123.38	123.51	123.26	123.53	122.81	124.58
C3—C5—C14	116.63	117.02	117.27	116.95	116.77	117.06	113.56	116.49
C5—C6—C13	126.11	126.38	127.05	127.3	128.21	128.13	124.67	127.95
N3—C8—C9	129.46	129.46	130.3	129.39	128.89	129.36	127.44	129.05
C8—C9—C10	117.72	117.36	116.33	117.23	116.79	117.33	117.8	117.5
C11—C12—C13	119.32	119.25	119.27	119.23	119.3	119.27	121.22	119.4
C8—C13—C12	118.38	118.46	118.76	118.26	118.05	118.25	115.79	117.89
N1—C15—C16	116.39	115.93	115.35	116.05	115.28	115.6	112.54	115.9
C15—C16—C21	121.86	122.78	122.78	122.7	123.19	122.96	123.36	123.13
C17—C18—C19	120.25	120.42	118.75	119.26	120.87	121.15	120.37	120
C18—C19—C20	119.72	119.17	121.44	120.48	118.08	117.55	119.74	119.5
C7—N3—C8	108.7	108.64	108.71	108.76	107.66	108.67	108.45	108.71
O1—C2—N1	119.72	119.87	120.2	120.11	119.64	119.31	121.43	119.65
C2—C3—C4	120.05	118.47	119.13	118.56	118.19	118.57	117.32	117.47
N2—C4—C3	176.87	178.14	179.06	178.6	177.62	177.95	177.15	176.74
C6—C5—C14	119.09	120.11	119.7	120.09	119.35	120.6	121.99	120.49
C7—C6—C13	106.03	106.19	105.95	105.99	106.2	105.96	107.02	105.81
N3—C8—C13	108.03	107.89	107.53	107.74	107.94	107.76	108.21	107.92



C9—C10—C11	120.8	121.17	123.03	121.18	121.64	121.09	120.28	120.97
C6—C13—C8	106.57	106.84	106.37	106.96	106.85	106.91	105.18	106.76
C5—C14—C15	121.25	121.29	121.28	121.34	120.86	121.2	123.85	121.75
C14—C15—C16	122.35	123.01	123.23	122.79	122.84	123.34	126.3	123.14
C17—C16—C21	118.5	118.18	117.04	117.81	117.08	117.62	115.83	117.32
C19—C20—C21	120.05	120.53	118.84	119.49	121.03	121.5	118.56	119.5
O2—C19—C18							118.03	116.07
O2—C19—C20							122.22	124.42
C19—O2—C24							118.9	117.68
N3—C22—C23	113.35	113.71			112.2	112.83	111.49	113.27
C18—C19—C24					121.26	121.21		
C20—C19—C24					120.65	121.23		
Cl1—C19—C18			119.48	119.98				
Cl1—C19—C20			119.07	119.53				
RMSE	0.631619234		0.654972039		0.633425033		1.735699027	
Maximum difference	1.58		1.85		1.73		3.56	

**Table S3:** Hydrogen-bond geometry (Å, °) of compound **4a**.

<i>D</i> —H... <i>A</i>	<i>D</i> —H	H... <i>A</i>	<i>D</i> ... <i>A</i>	<i>D</i> —H... <i>A</i>
C9—H9...N2 <sup>i</sup>	1.08	2.47	3.397	143
C20—H20...O1 <sup>ii</sup>	1.08	2.50	3.0882	113
C19—H19...Cg3 <sup>iii</sup>	1.08	2.99	4.0098	157
C22—H22B...Cg1 <sup>i</sup>	1.08	2.64	3.6215	150
C23—H23C...Cg3 <sup>i</sup>	1.08	2.99	3.6617	120

Symmetry code: (i) -X, -1-Y, -1-Z; (ii) -1/2+X, -3/2-Y, Z; (iii) -1/2-X, -1/2+Y, -Z.

Cg1: N3—C7—C6—C13—C8.

Cg3: C8—C9—C10—C11—C12—C13.

**Table S4:**  $\pi$ -bond geometry (Å, °) of compound **4b**.

<i>Y</i> — <i>X</i> ... <i>Cg</i>	<i>Y</i> — <i>X</i>	<i>X</i> ... <i>Cg</i>	<i>Y</i> ... <i>Cg</i>	<i>Y</i> — <i>X</i> ... <i>Cg</i>
C19—C1...Cg3 <sup>i</sup>	1.7461	3.7892	5.4677	161
C4—N2...Cg4 <sup>ii</sup>	1.1456	3.9789	4.5246	111

Symmetry code: (i) 4-X, 3-Y, -Z; (ii) -5-X, -3-Y, 1-Z.

Cg3: C8—C9—C10—C11—C12—C13.

Cg4: C16—C17—C18—C19—C20—C21.

**Table S5:** Hydrogen-bond geometry (Å, °) of compound **4c**.

<i>D</i> —H... <i>A</i>	<i>D</i> —H	H... <i>A</i>	<i>D</i> ... <i>A</i>	<i>D</i> —H... <i>A</i>
C20—H201...O1 <sup>ii</sup>	0.95	2.646	3.477	146

Symmetry code: (i) X, ½-Y, -½+Z.

**Table S6:** Hydrogen-bond geometry (Å, °) of compound **4d**.

<i>C</i> —H... <i>Cg</i>	<i>C</i> —H	H... <i>Cg</i>	<i>C</i> ... <i>Cg</i>	<i>C</i> —H... <i>Cg</i>
C1—H12... <i>Cg1</i> <sup>i</sup>	0.94	2.96	3.8764	165
C22—H222... <i>Cg1</i> <sup>ii</sup>	0.99	2.91	3.5889	127

Symmetry code: (i) -3-X, 4-Y, -2-Z; (ii) -4-X, 4-Y, -2-Z.

*Cg1*: N3—C7—C6—C13—C8.

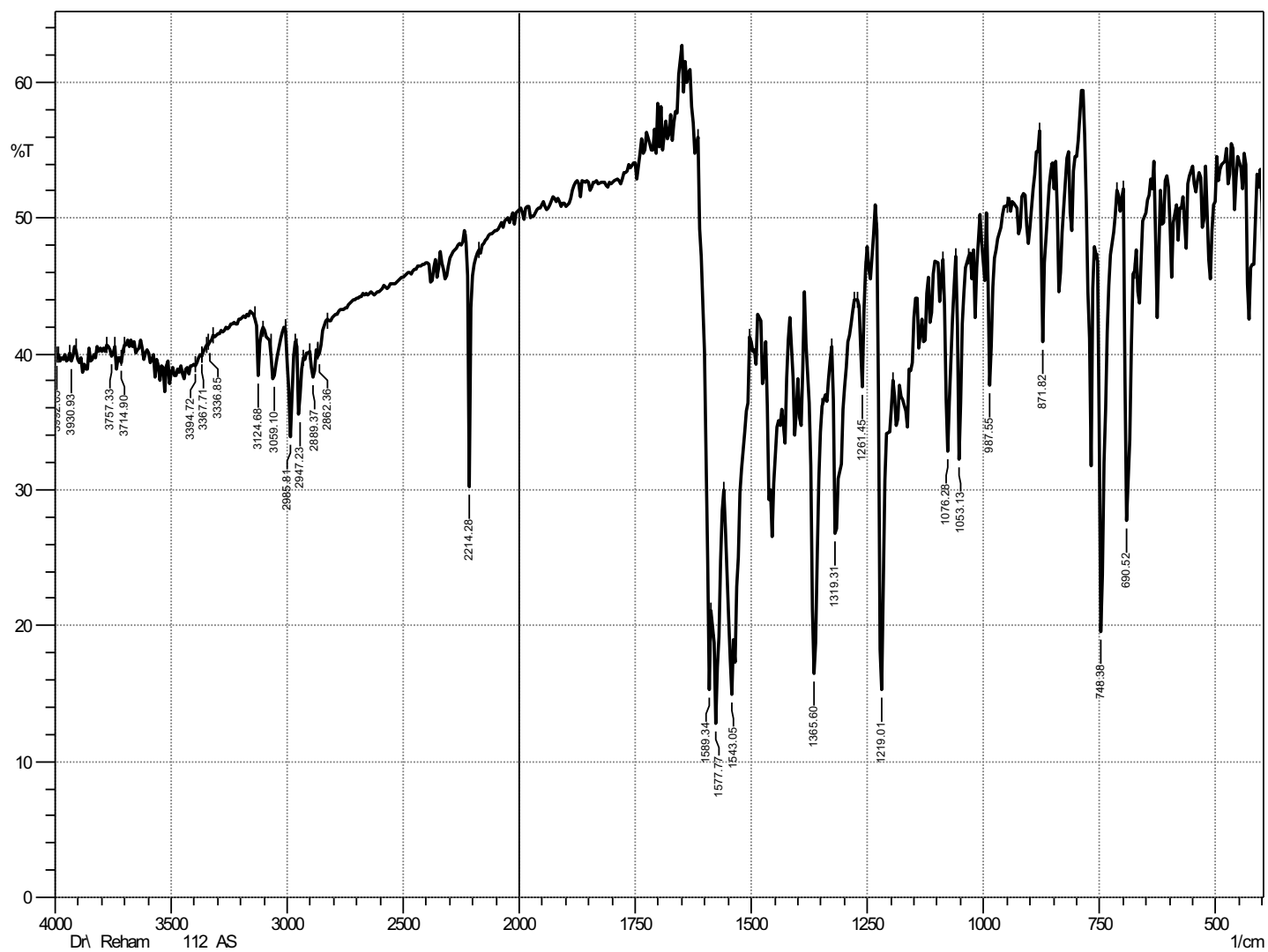


**Fig. S1.** IR spectrum of compound **4a** (KBr pellet).

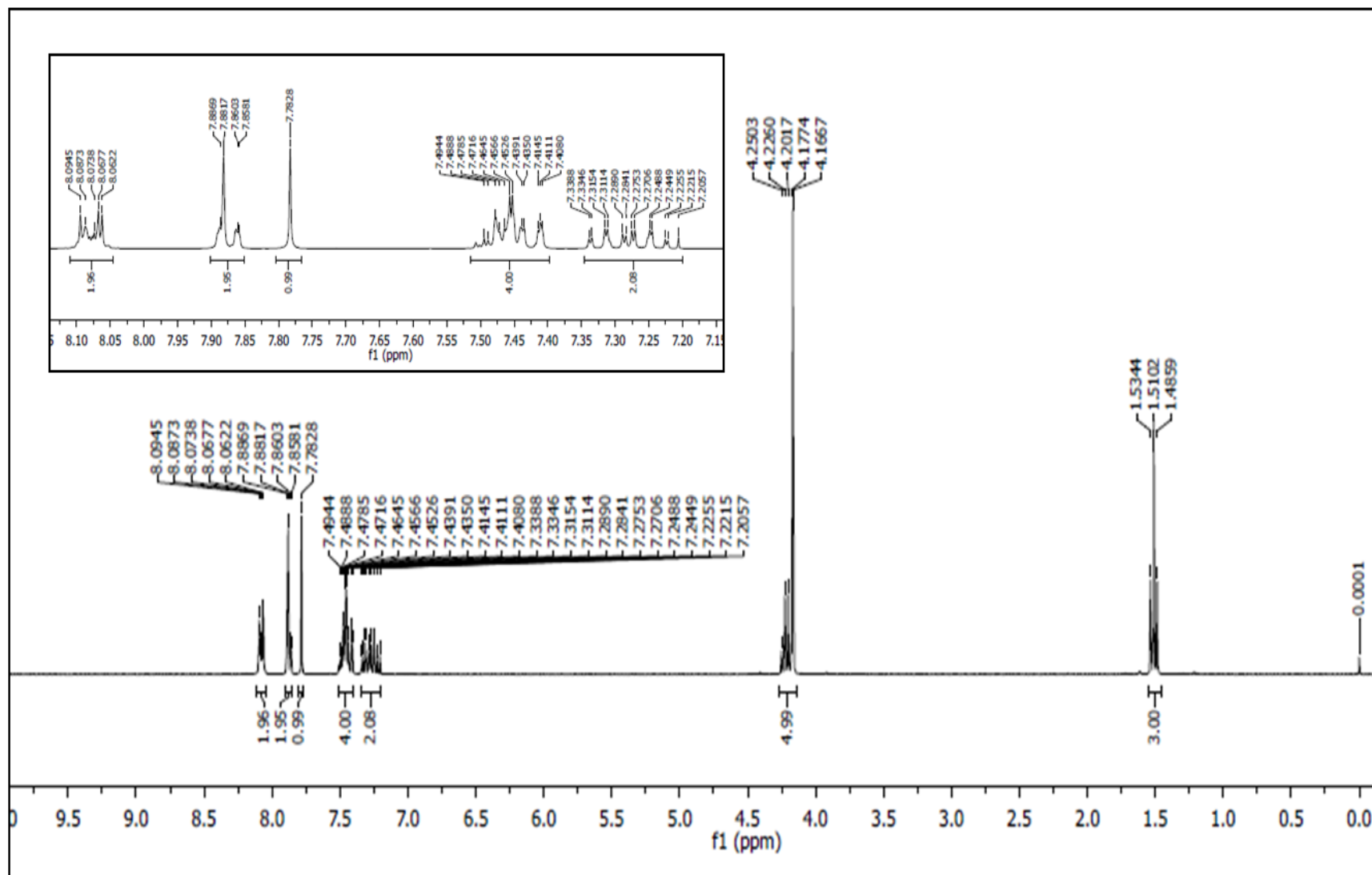


**Fig. S2.**  $^1\text{H}$ -NMR spectrum of compound **4a** in  $\text{CDCl}_3$ .

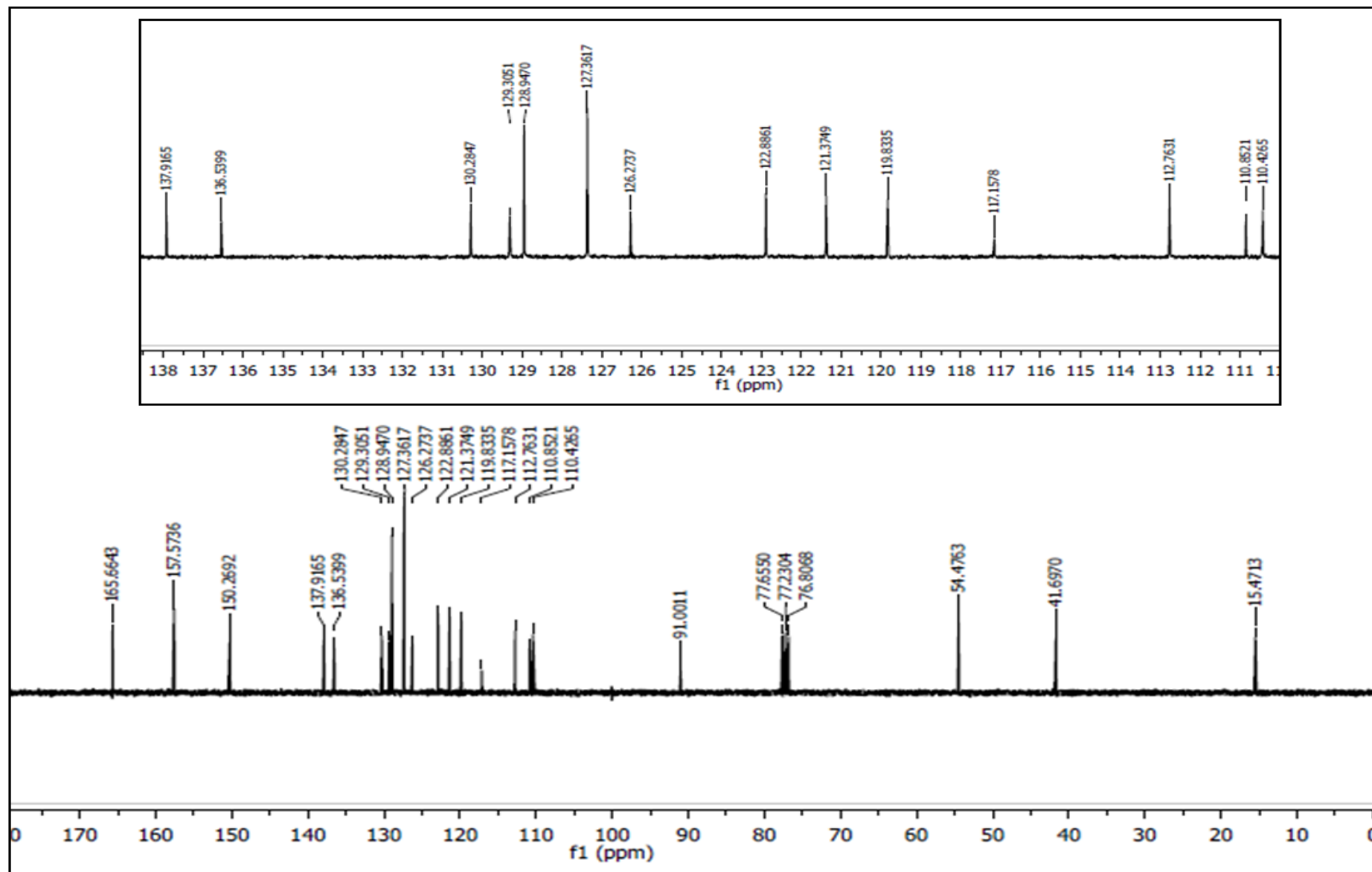


**Fig. S3.**  $^{13}\text{C}$ -NMR spectrum of compound **4a** in  $\text{CDCl}_3$ .

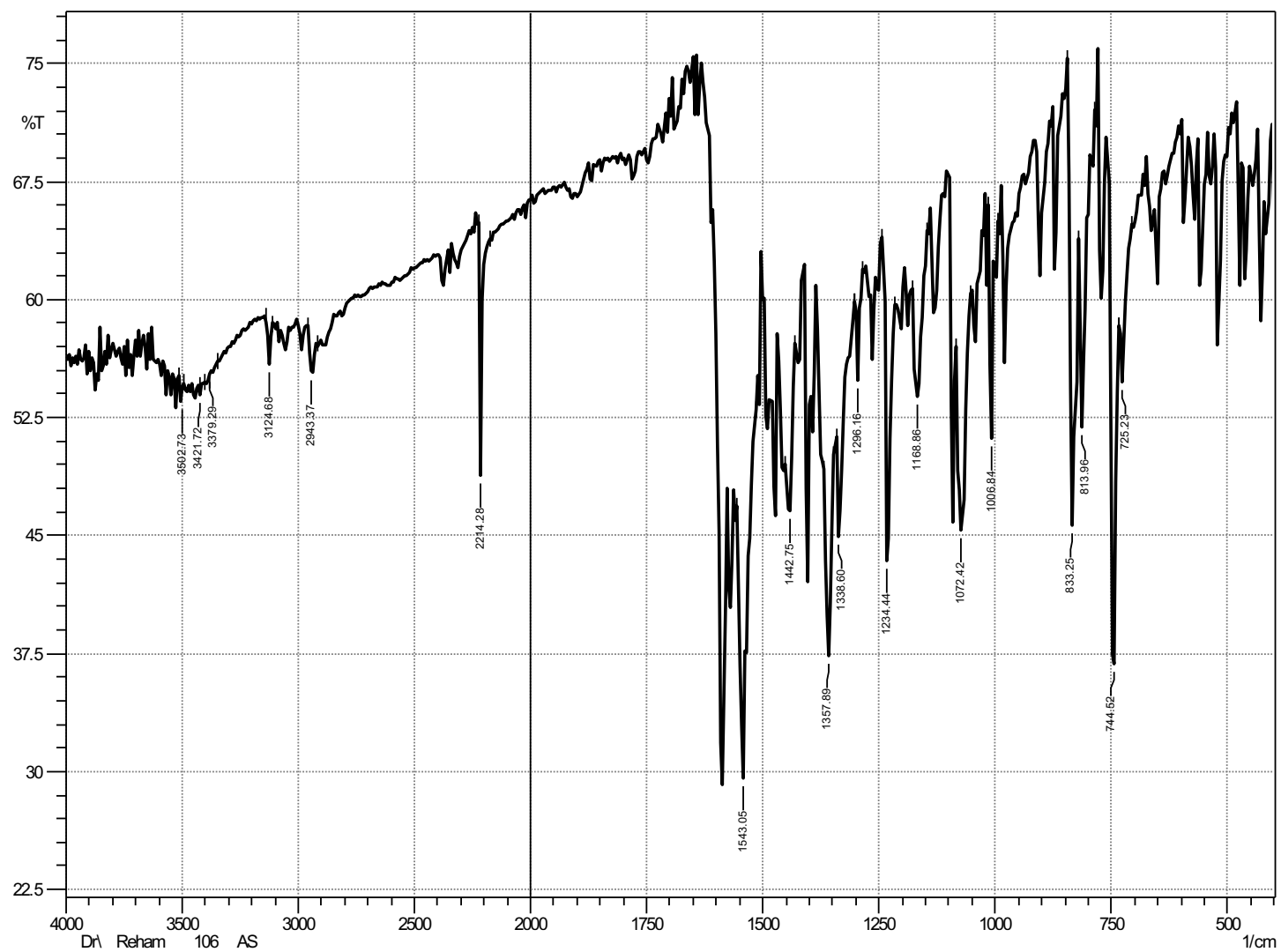


**Fig. S4.** IR spectrum of compound **4b** (KBr pellet).

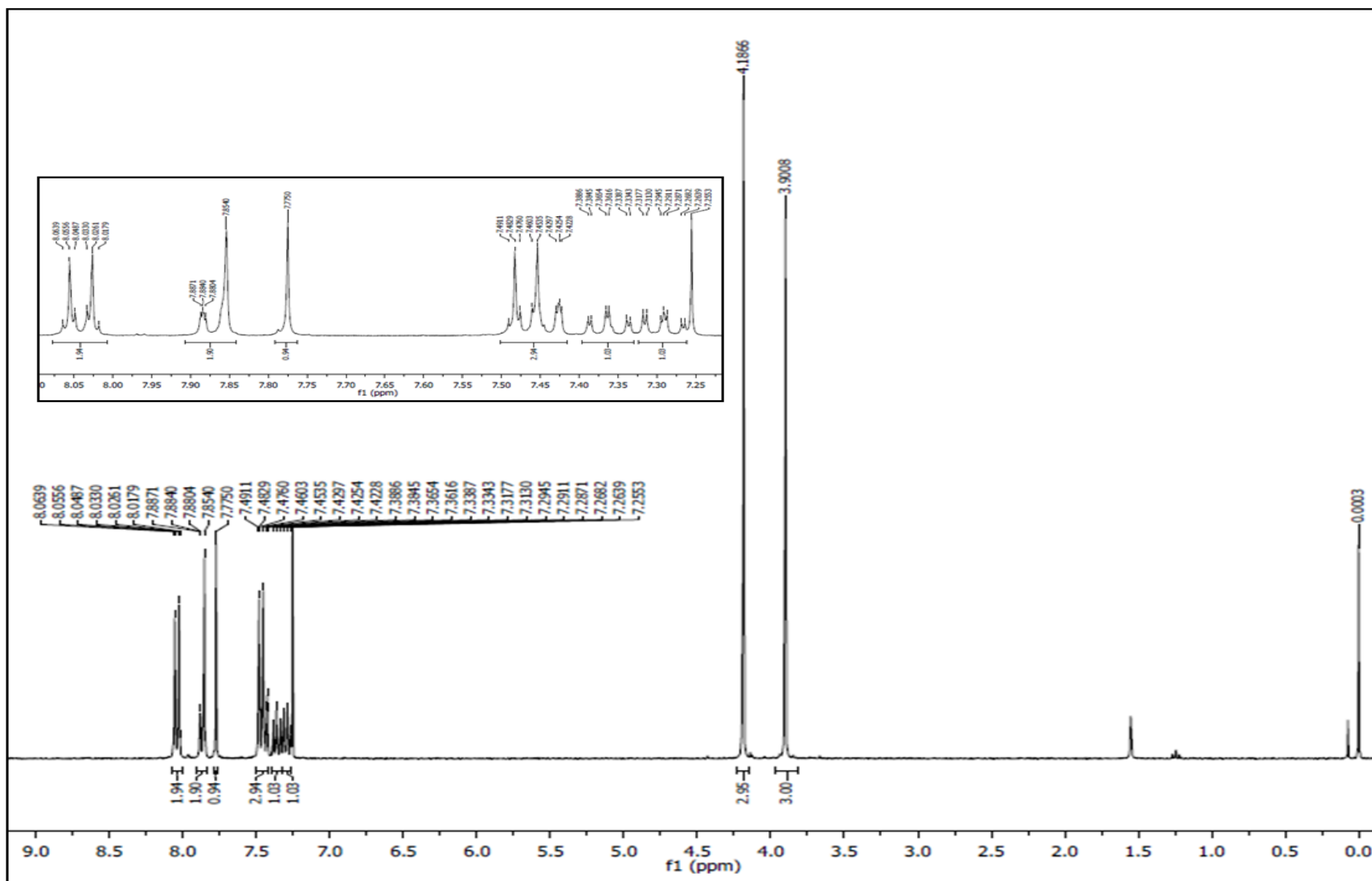


**Fig. S5.**  $^1\text{H}$ -NMR spectrum of compound **4b** in  $\text{CDCl}_3$ .



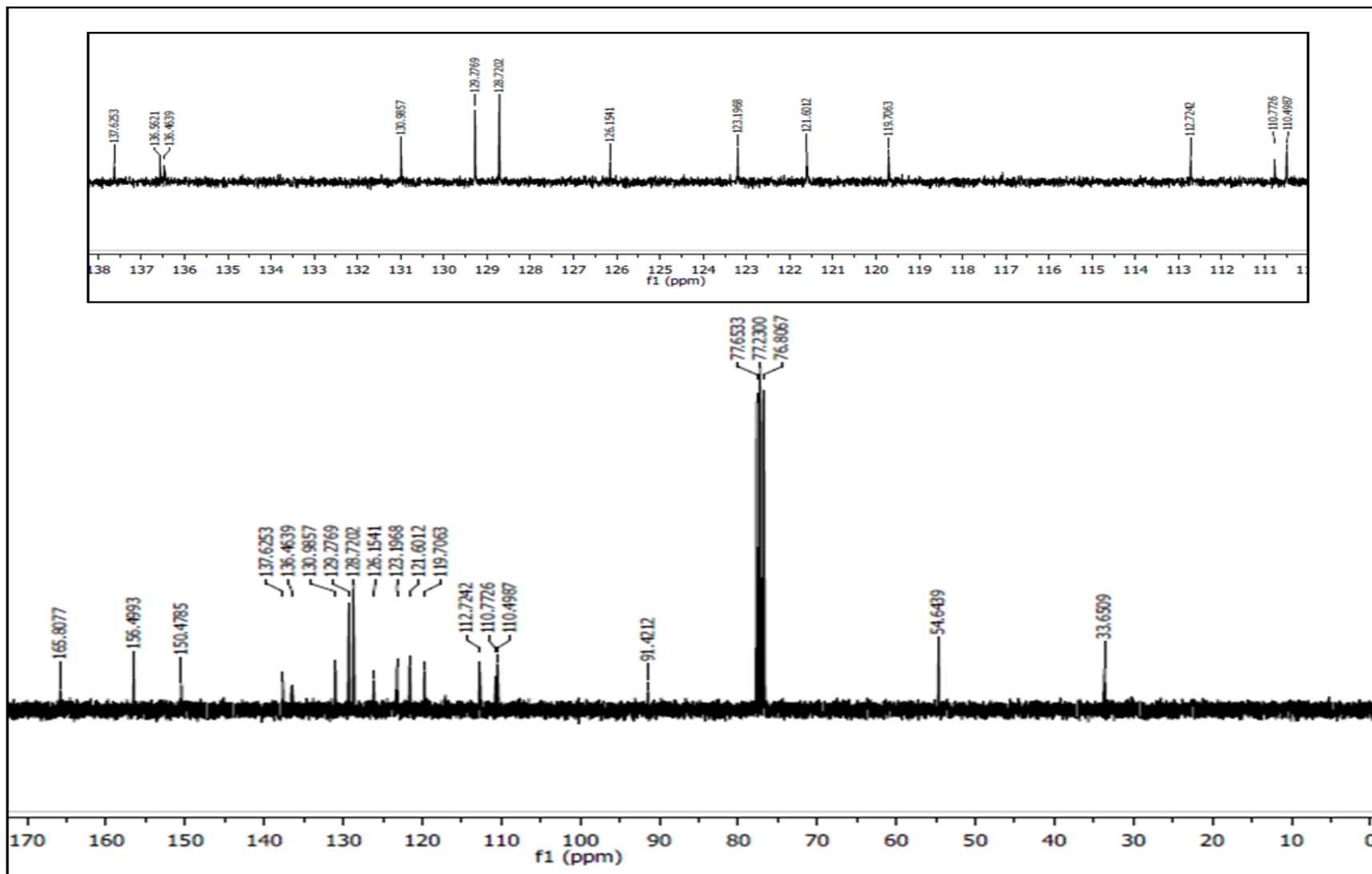


Fig. S6.  $^{13}\text{C}$ -NMR spectrum of compound **4b** in  $\text{CDCl}_3$ .

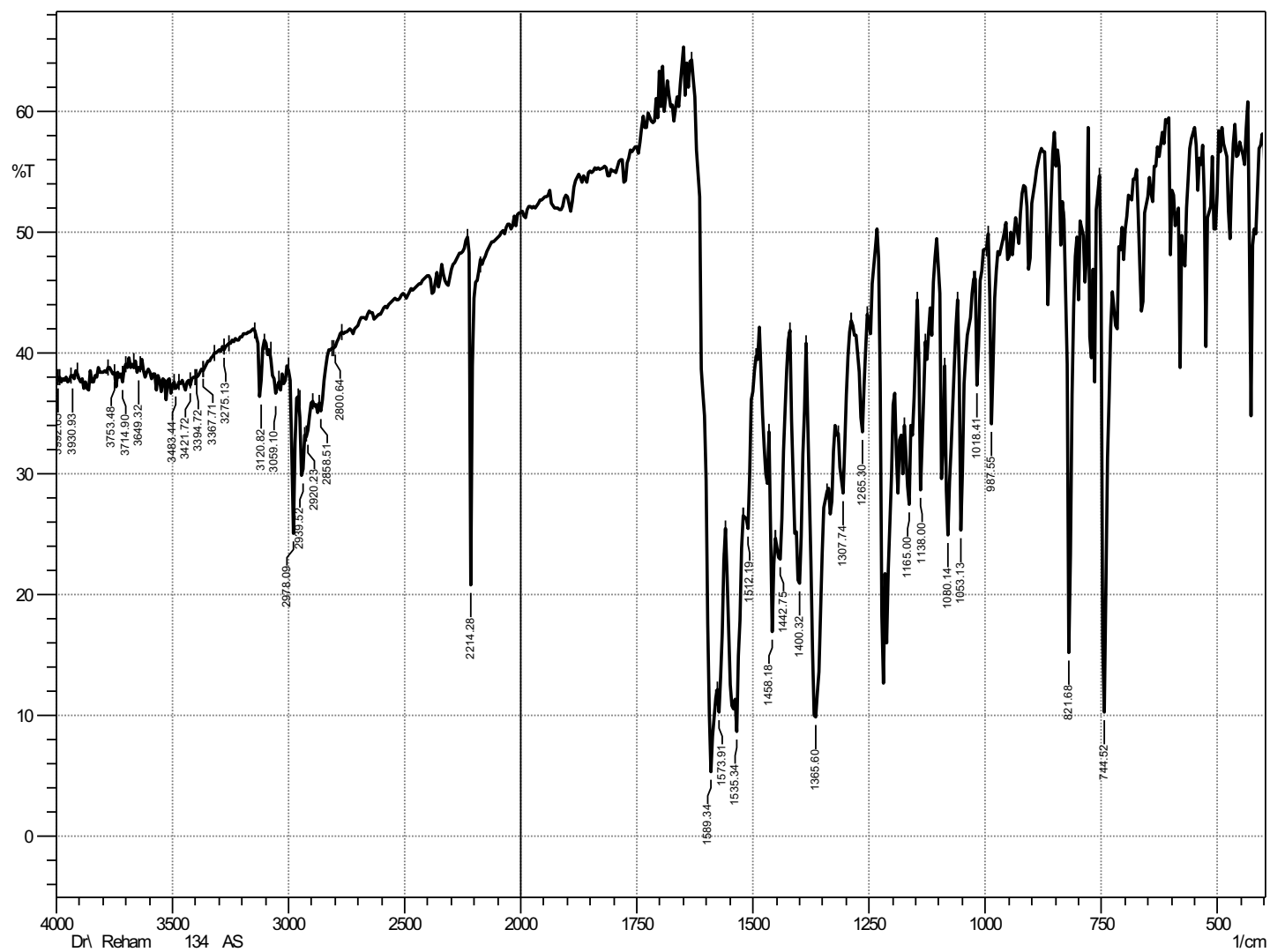


Fig. S7. IR spectrum of compound 4c (KBr pellet).

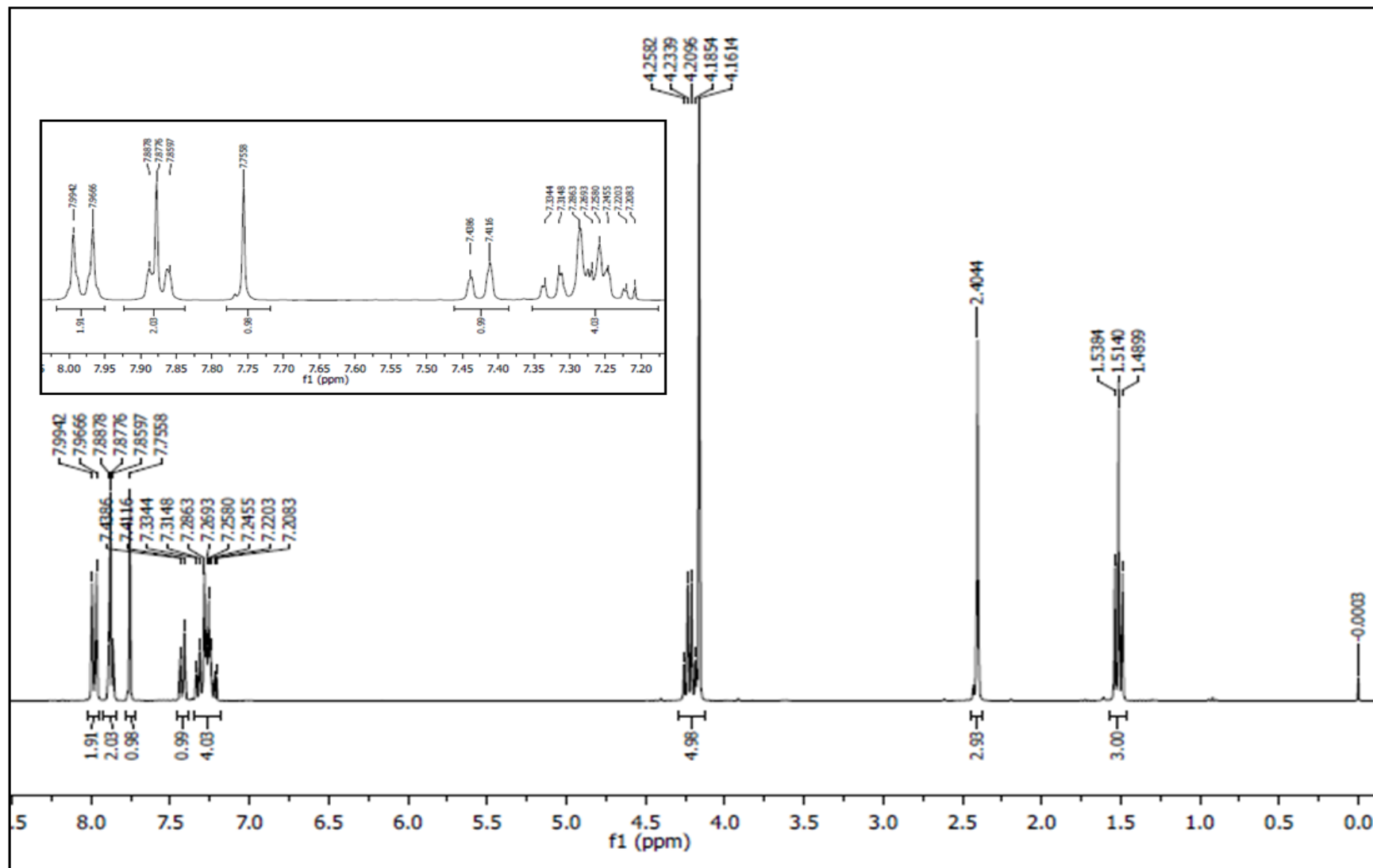
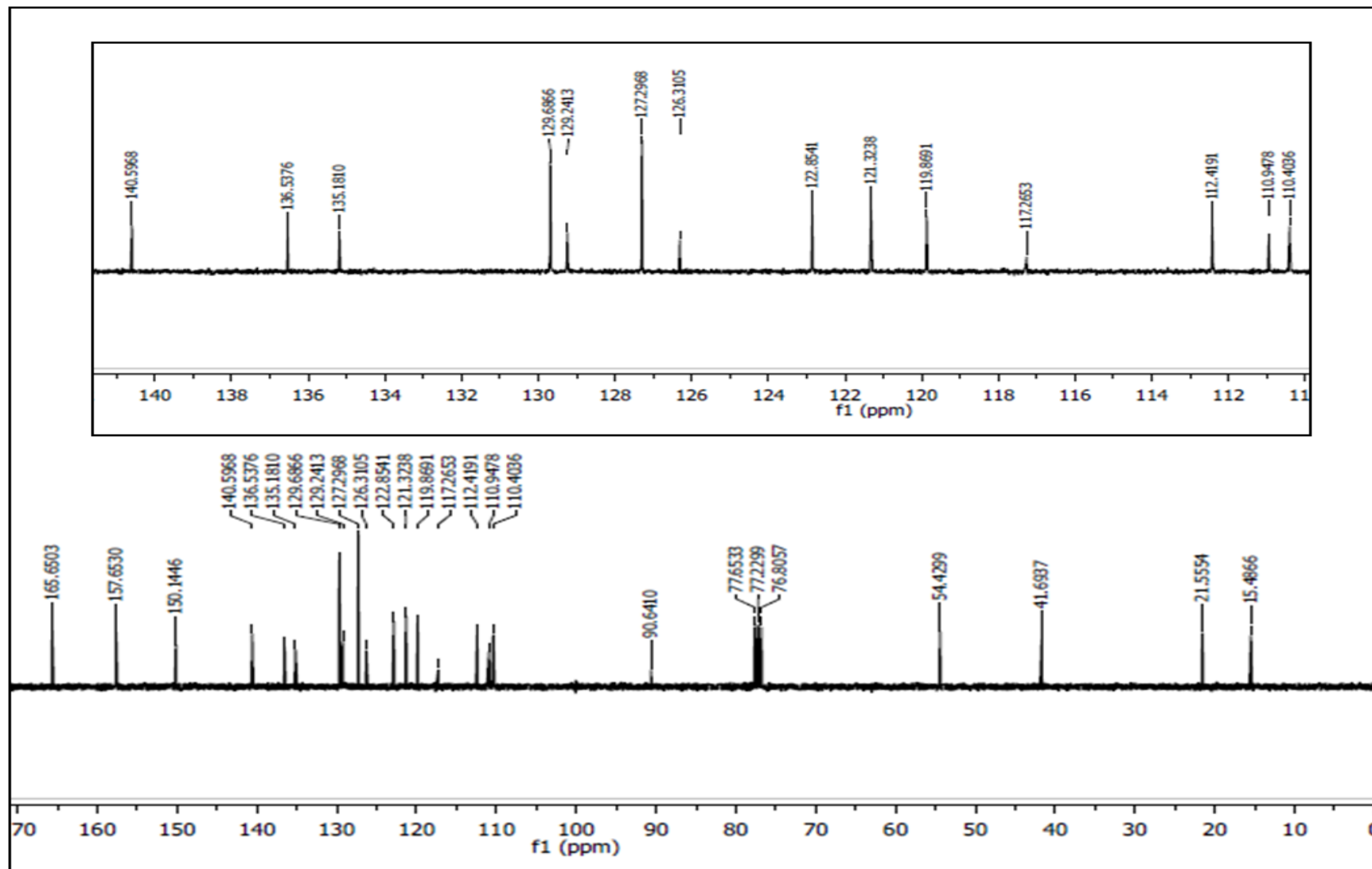
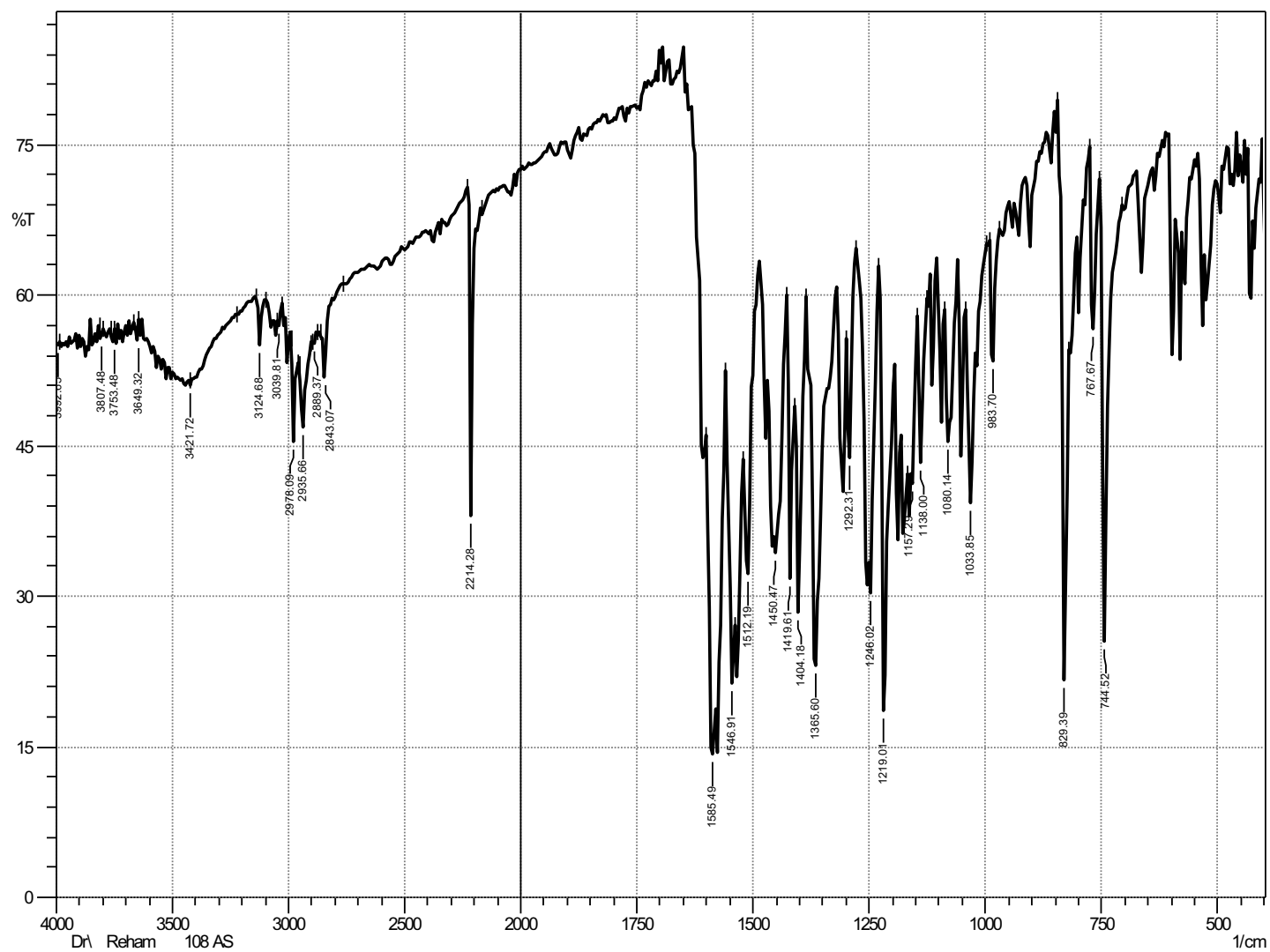


Fig. S8.  $^1\text{H}$ -NMR spectrum of compound **4c** in  $\text{CDCl}_3$ .



**Fig. S9.**  $^{13}\text{C}$ -NMR spectrum of compound **4c** in  $\text{CDCl}_3$ .



**Fig. S10.** IR spectrum of compound **4d** (KBr pellet).

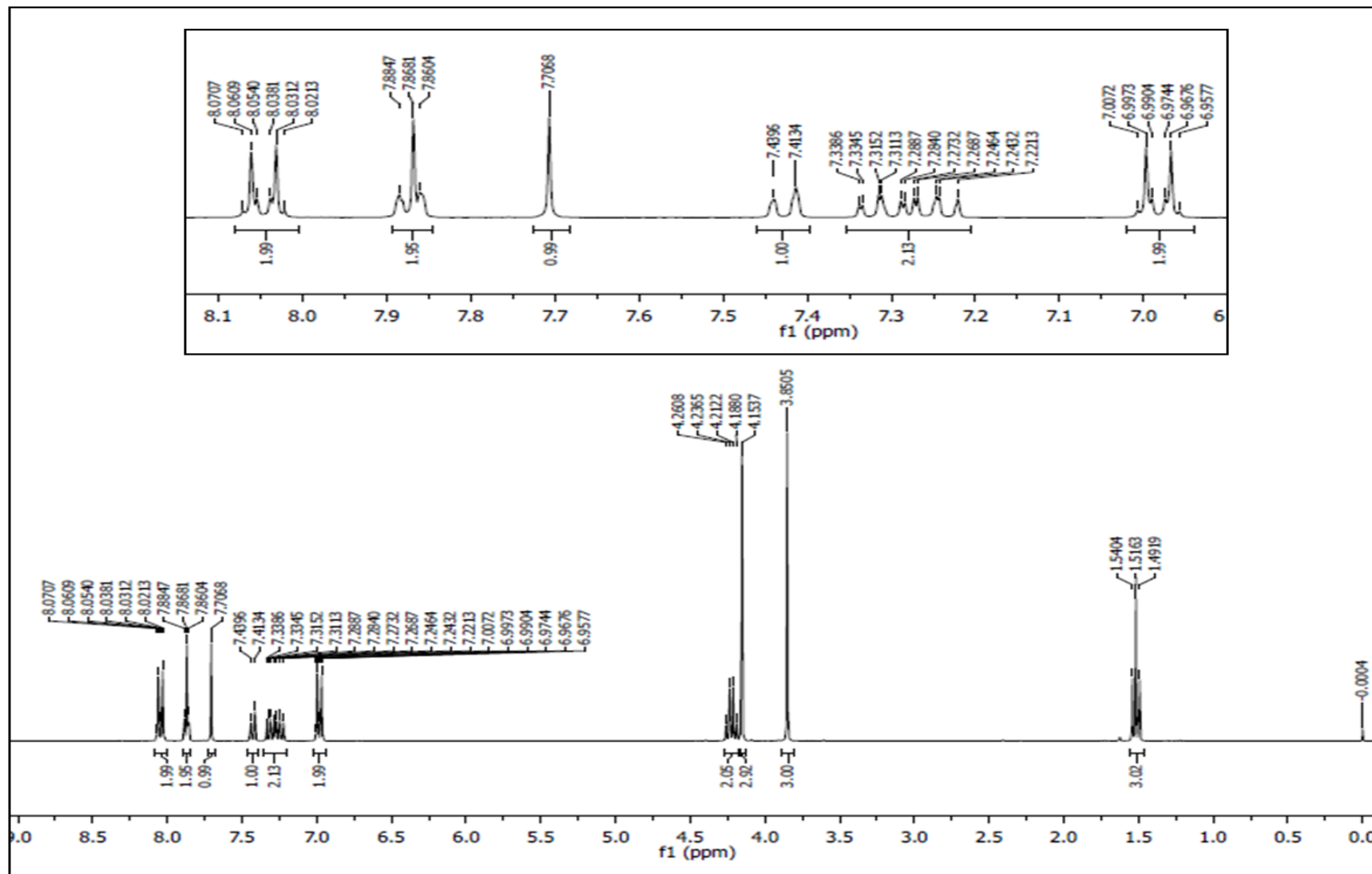


Fig. S11.  $^1\text{H}$ -NMR spectrum of compound **4d** in  $\text{CDCl}_3$ .

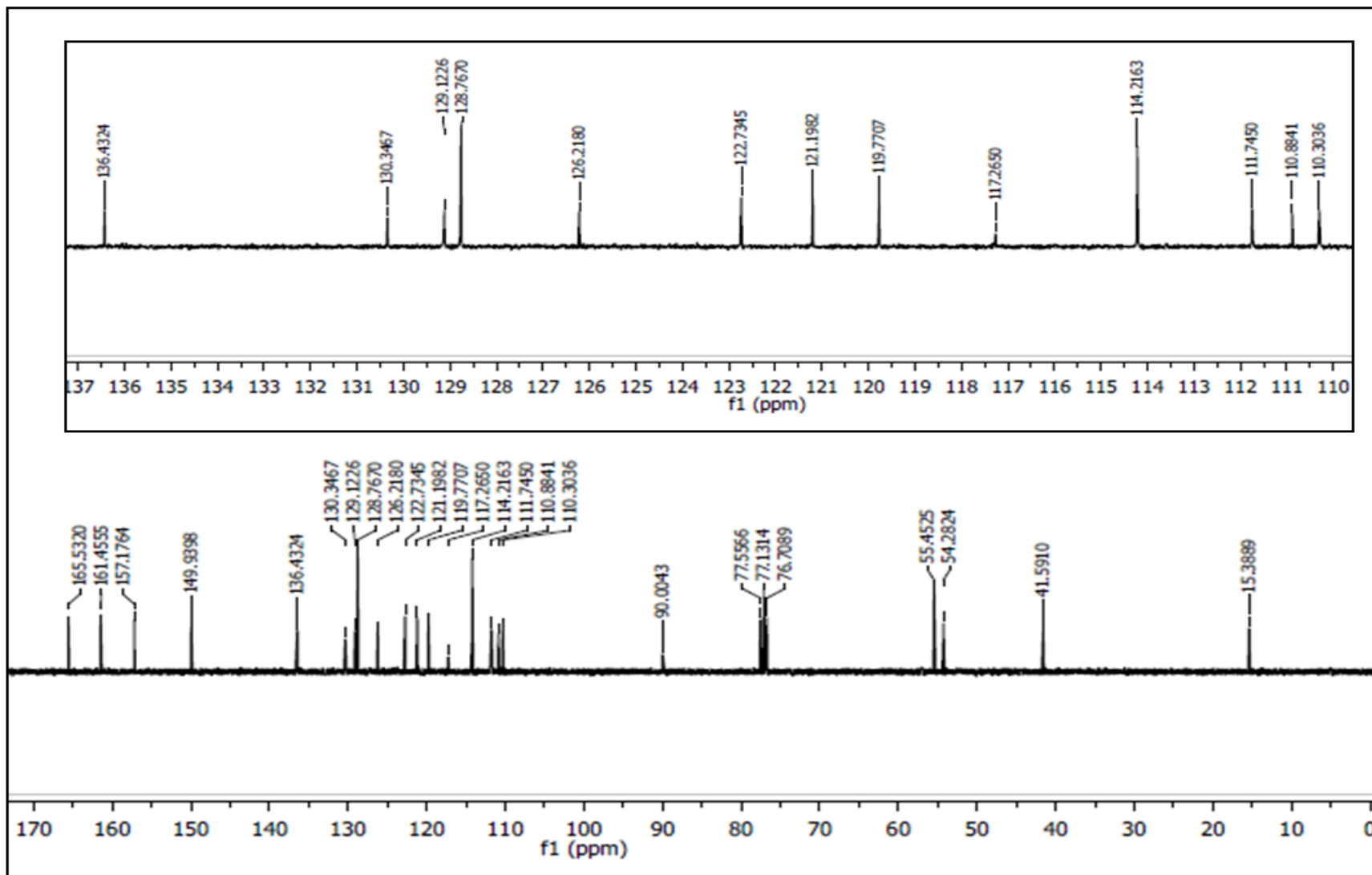
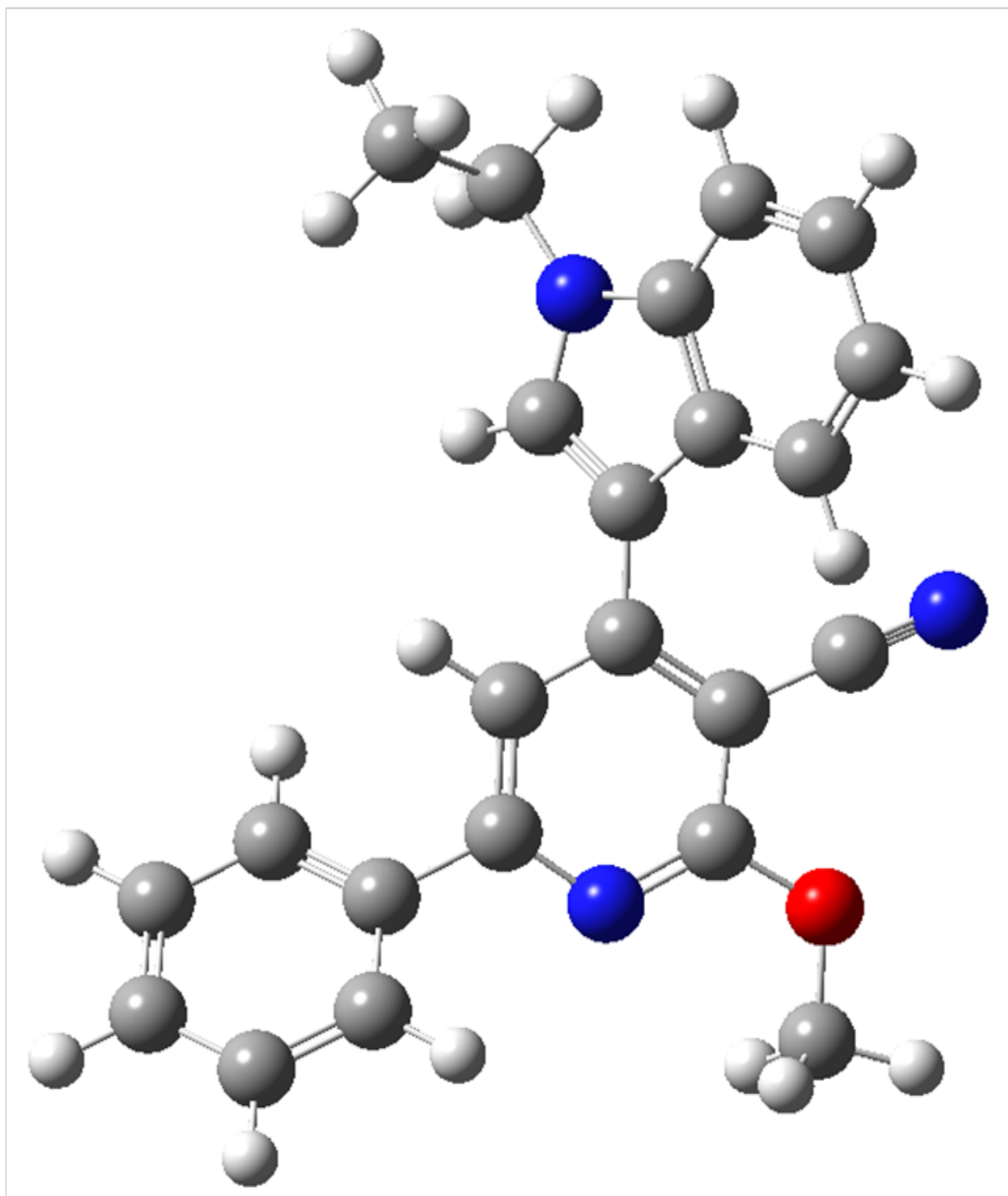
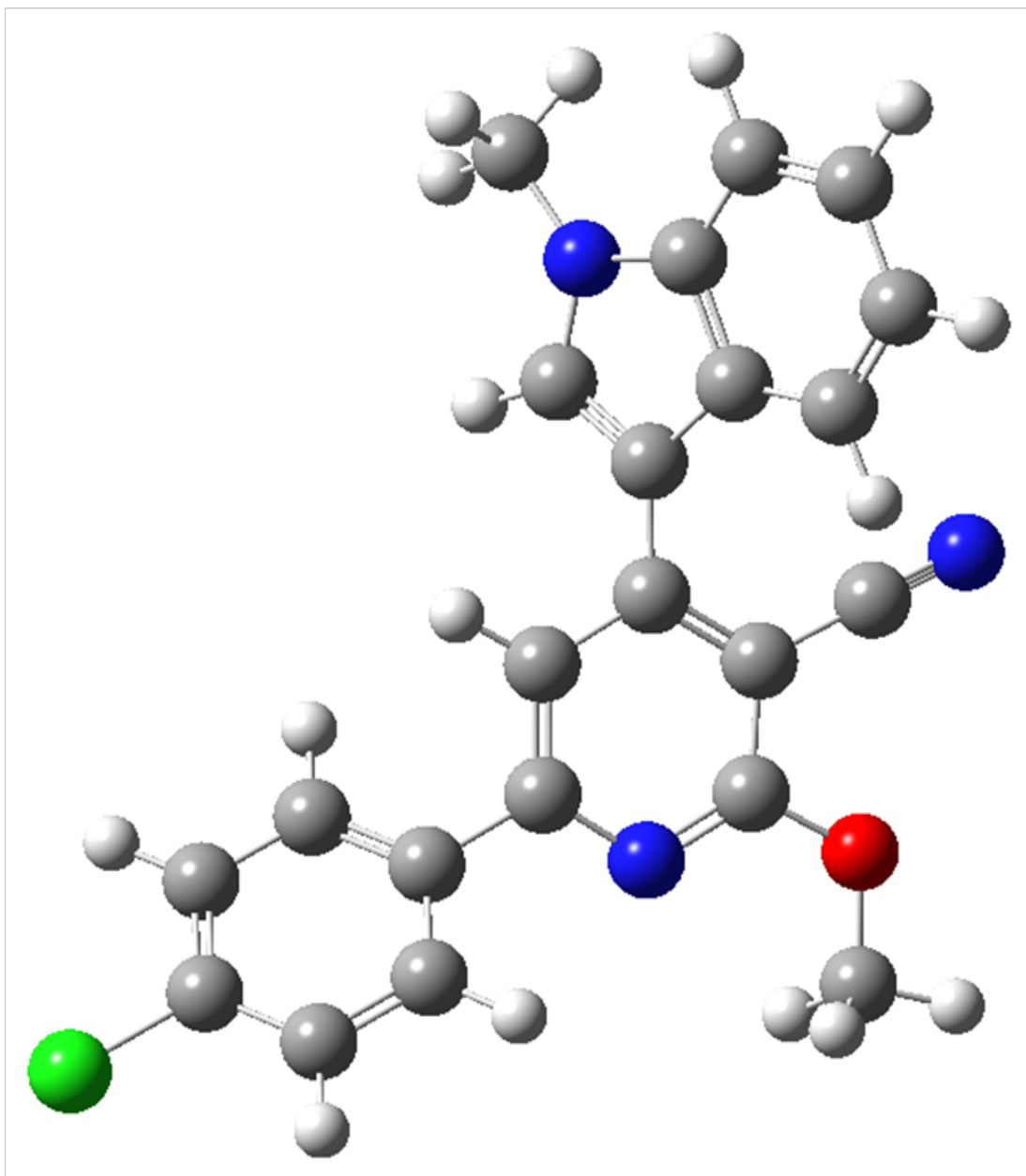


Fig. S12.  $^{13}\text{C}$ -NMR spectrum of compound **4d** in  $\text{CDCl}_3$ .



**Fig. S13.** A projection of the optimized structure of compound **4a** by DFT/B3LYP method with 6-31G(d,p) basis set.





**Fig. S14.** A projection of the optimized structure of compound **4b** by DFT/B3LYP method with 6-31G(d,p) basis set.

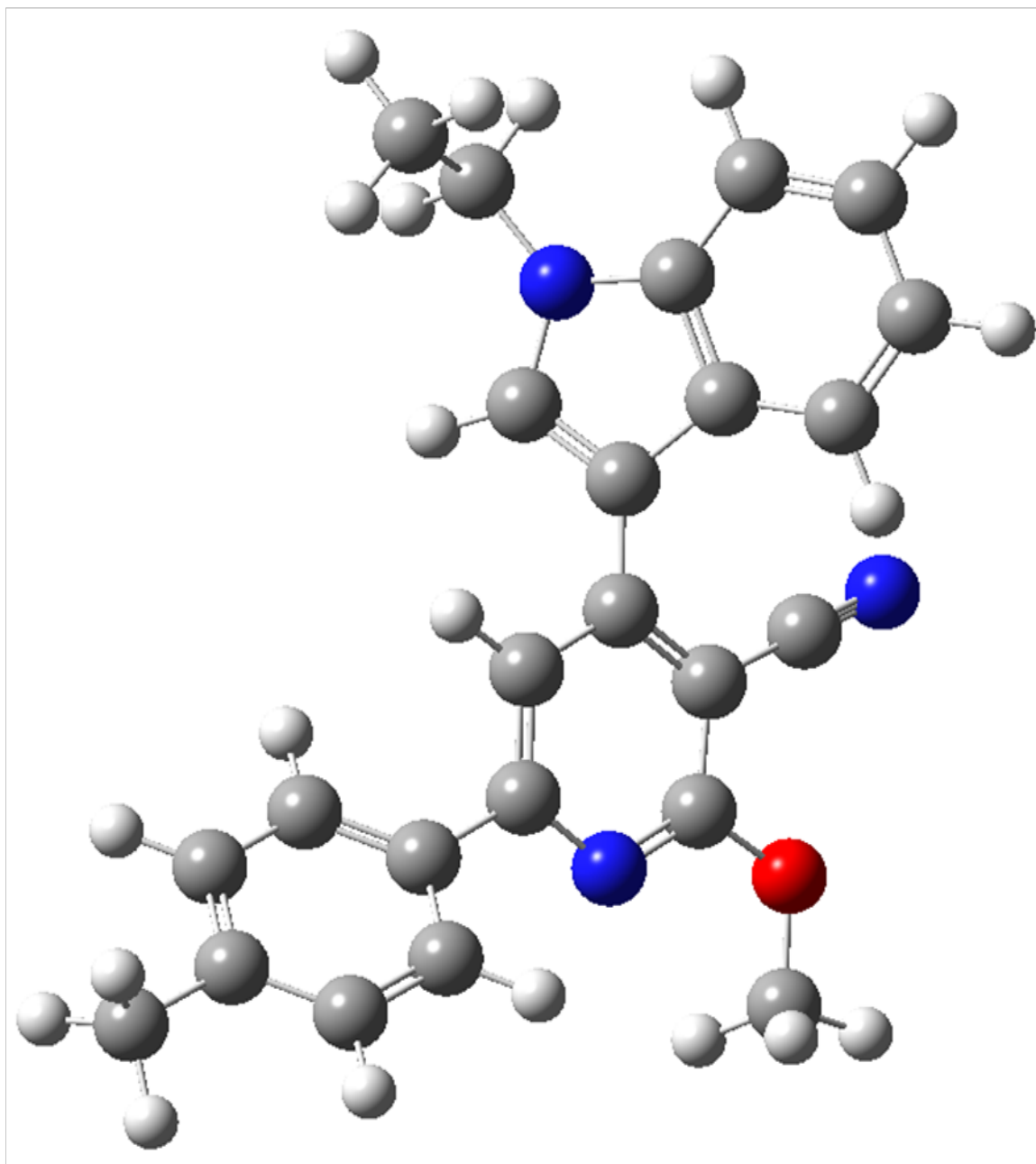


**Fig. S15.** A projection of the optimized structure of compound **4c** by DFT/B3LYP method with 6-31G(d,p) basis set.

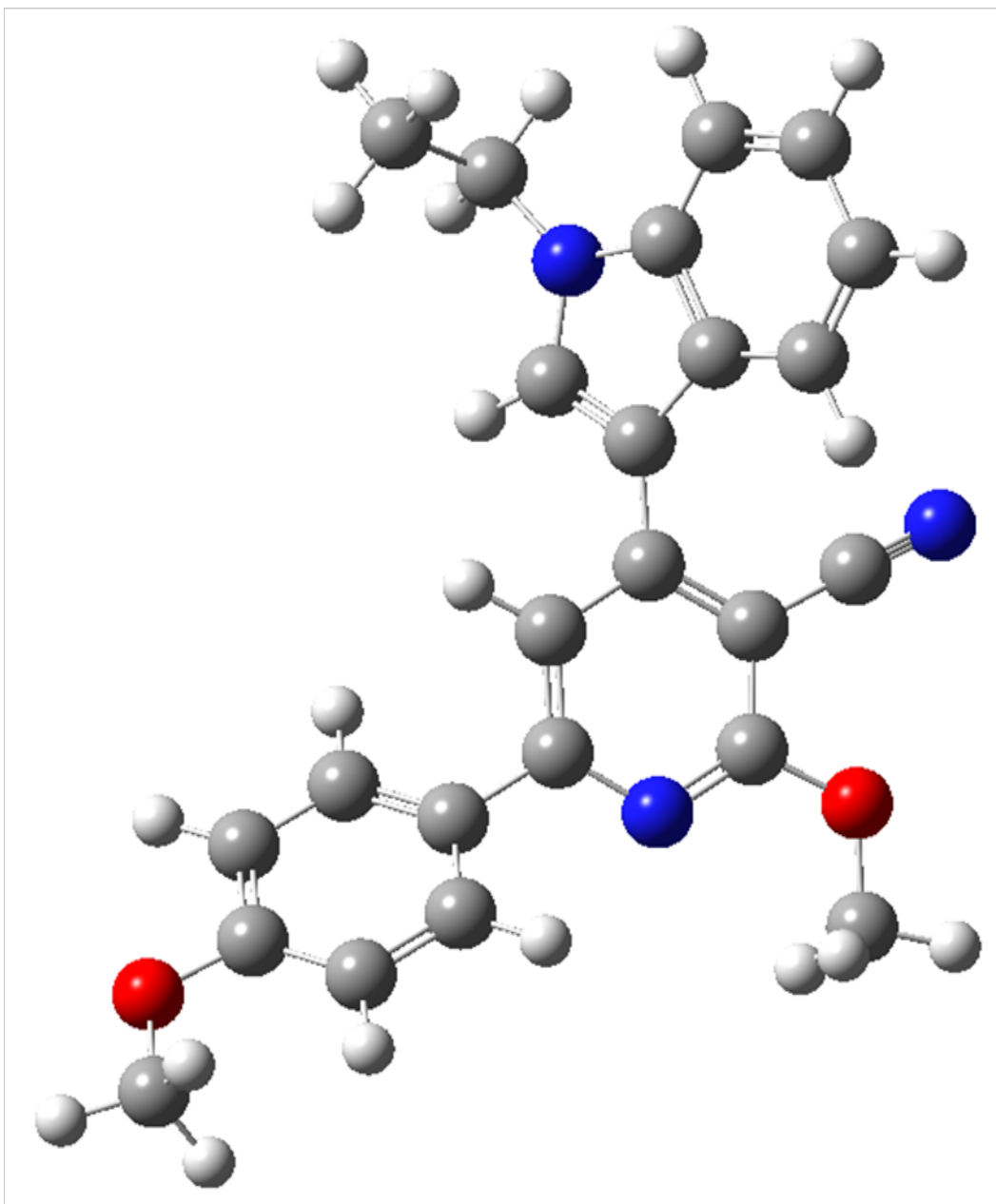


**Fig. S16.** A projection of the optimized structure of compound **4d** by DFT/B3LYP method with 6-31G(d,p) basis set.

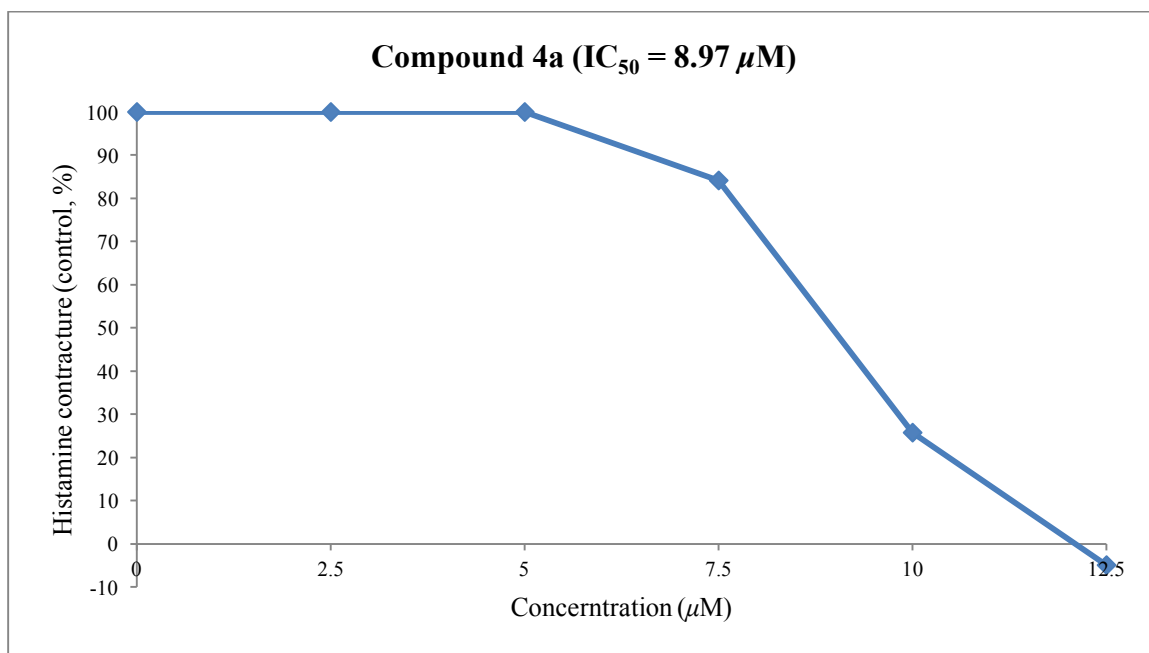


**Fig. S17.** Effect of compound **4a** on contracture induced by histamine in isolated guinea pig tracheal rings.

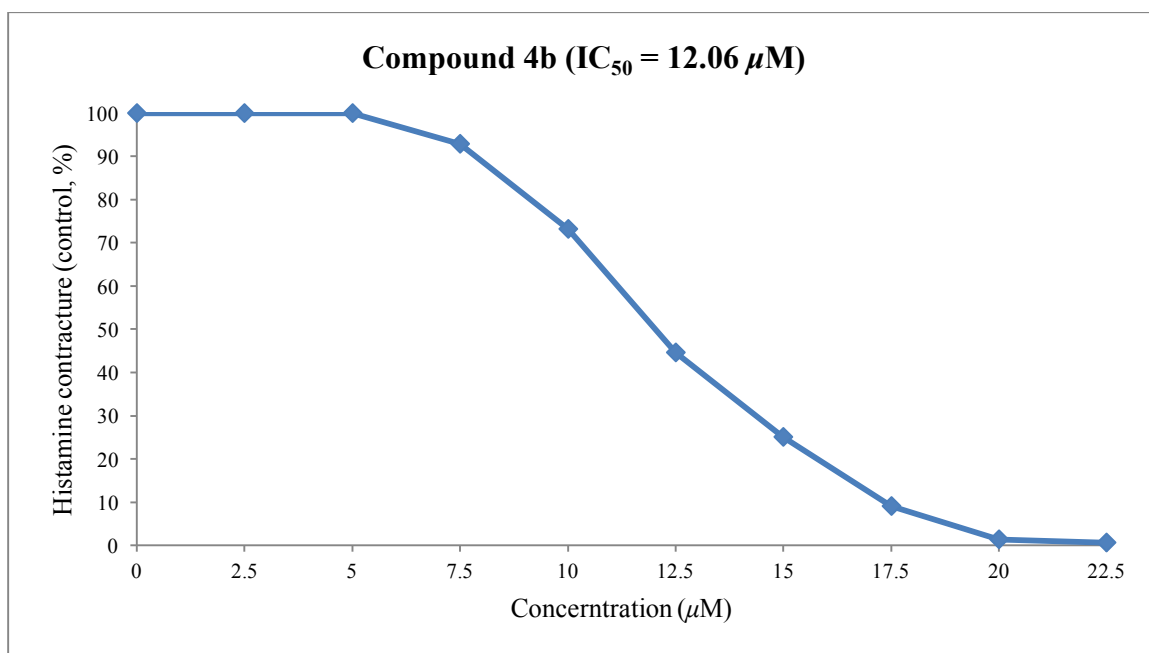


**Fig. S18.** Effect of compound **4b** on contracture induced by histamine in isolated guinea pig tracheal rings.

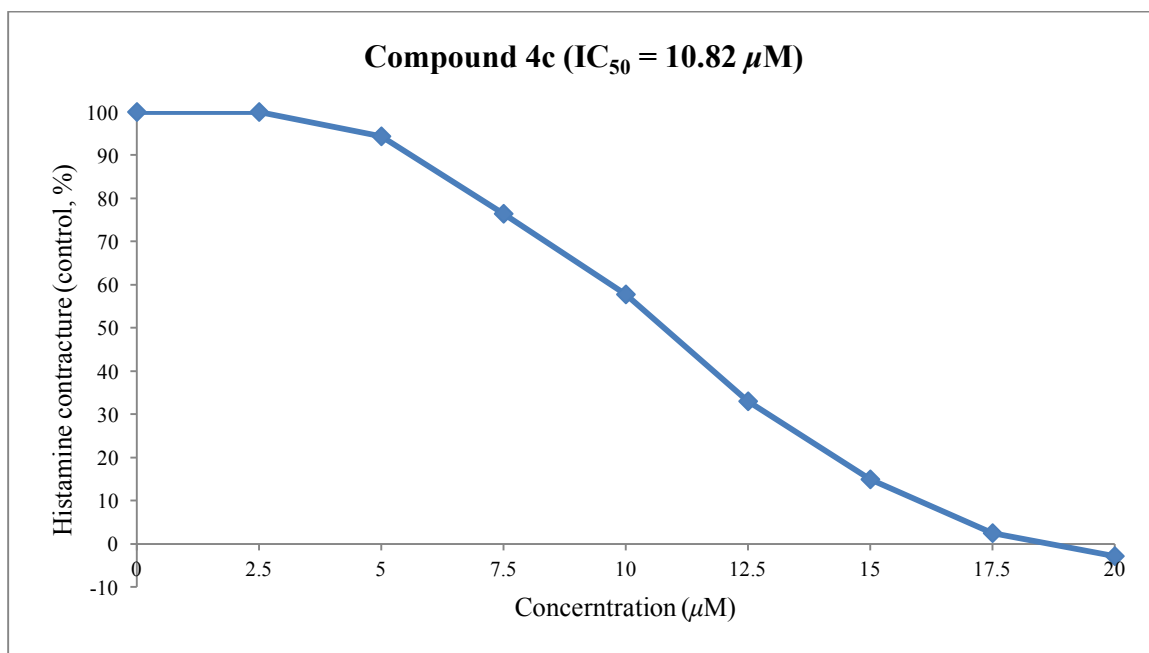


**Fig. S19.** Effect of compound **4c** on contracture induced by histamine in isolated guinea pig tracheal rings.

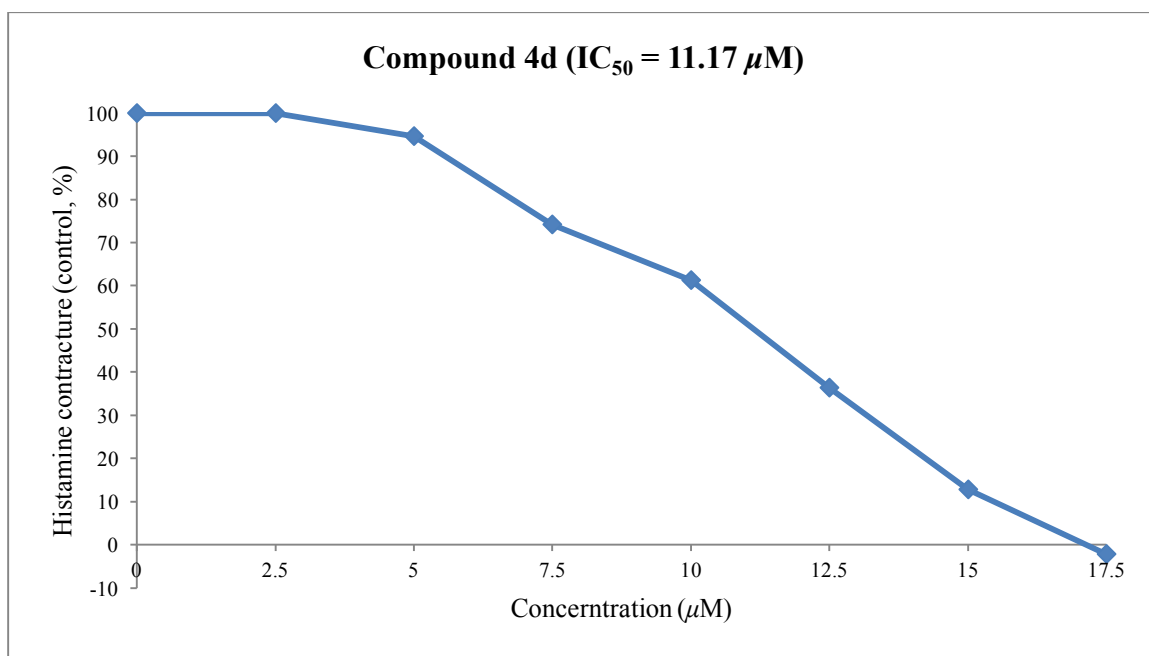


**Fig. S20.** Effect of compound **4d** on contracture induced by histamine in isolated guinea pig tracheal rings.

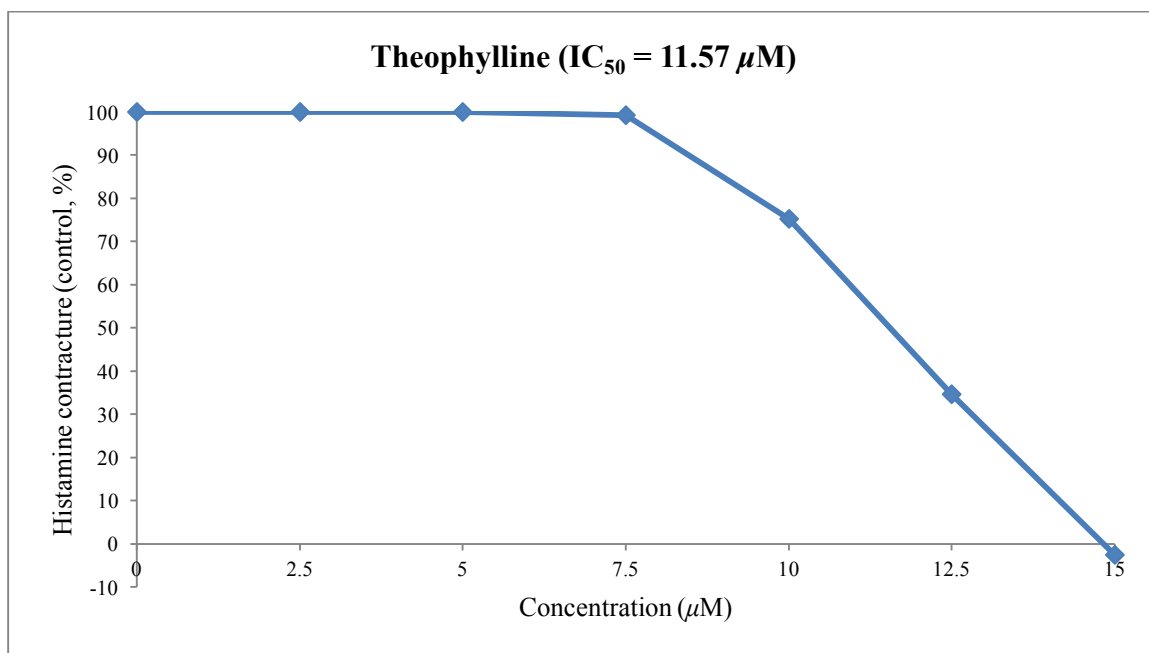


**Fig. S21.** Effect of theophylline on contracture induced by histamine in isolated guinea pig tracheal rings.

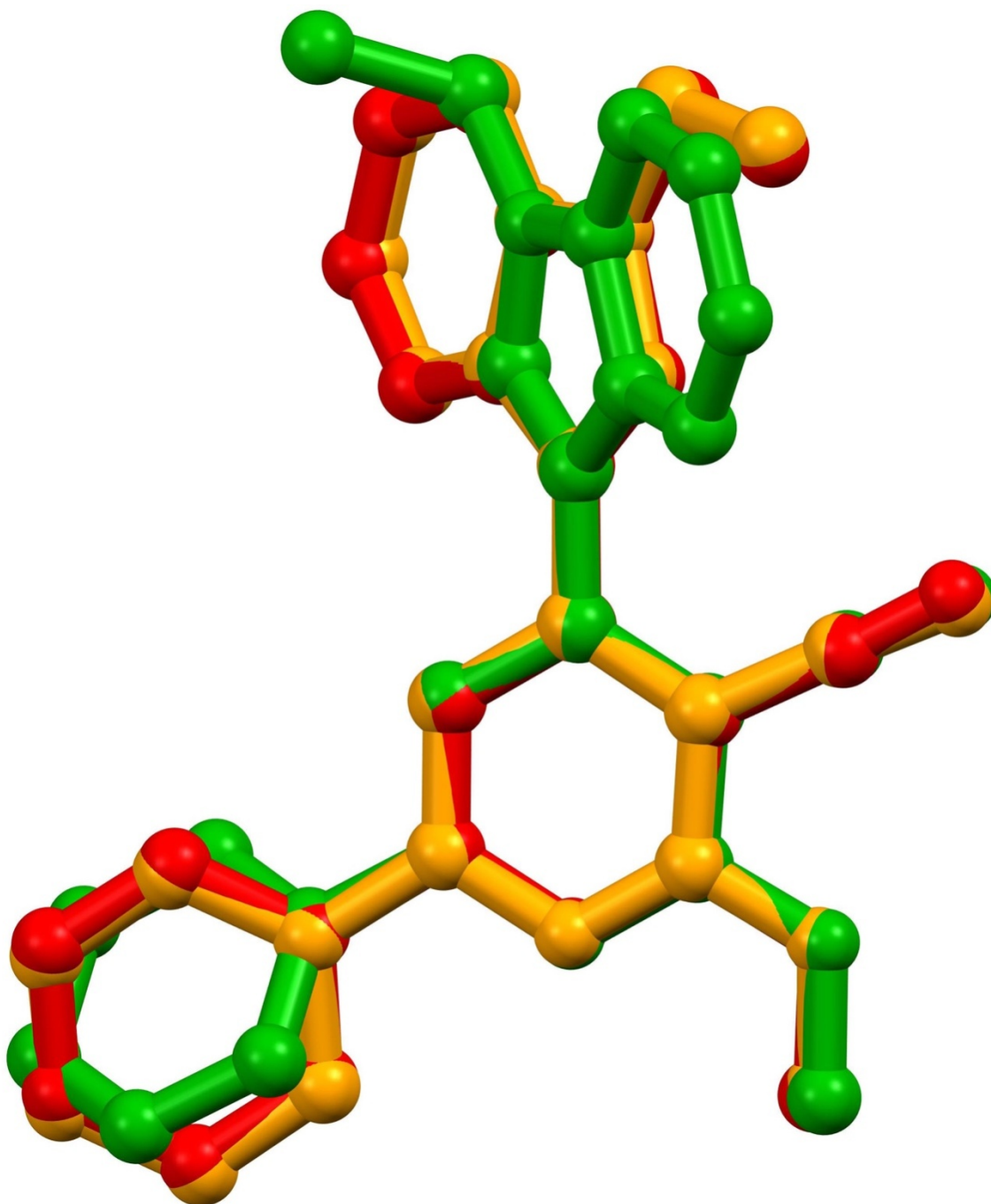


**Fig. S22.** Overlay view of compound **4a**, red (X-ray structure), green (free state DFT), yellow (DFT-d validation).

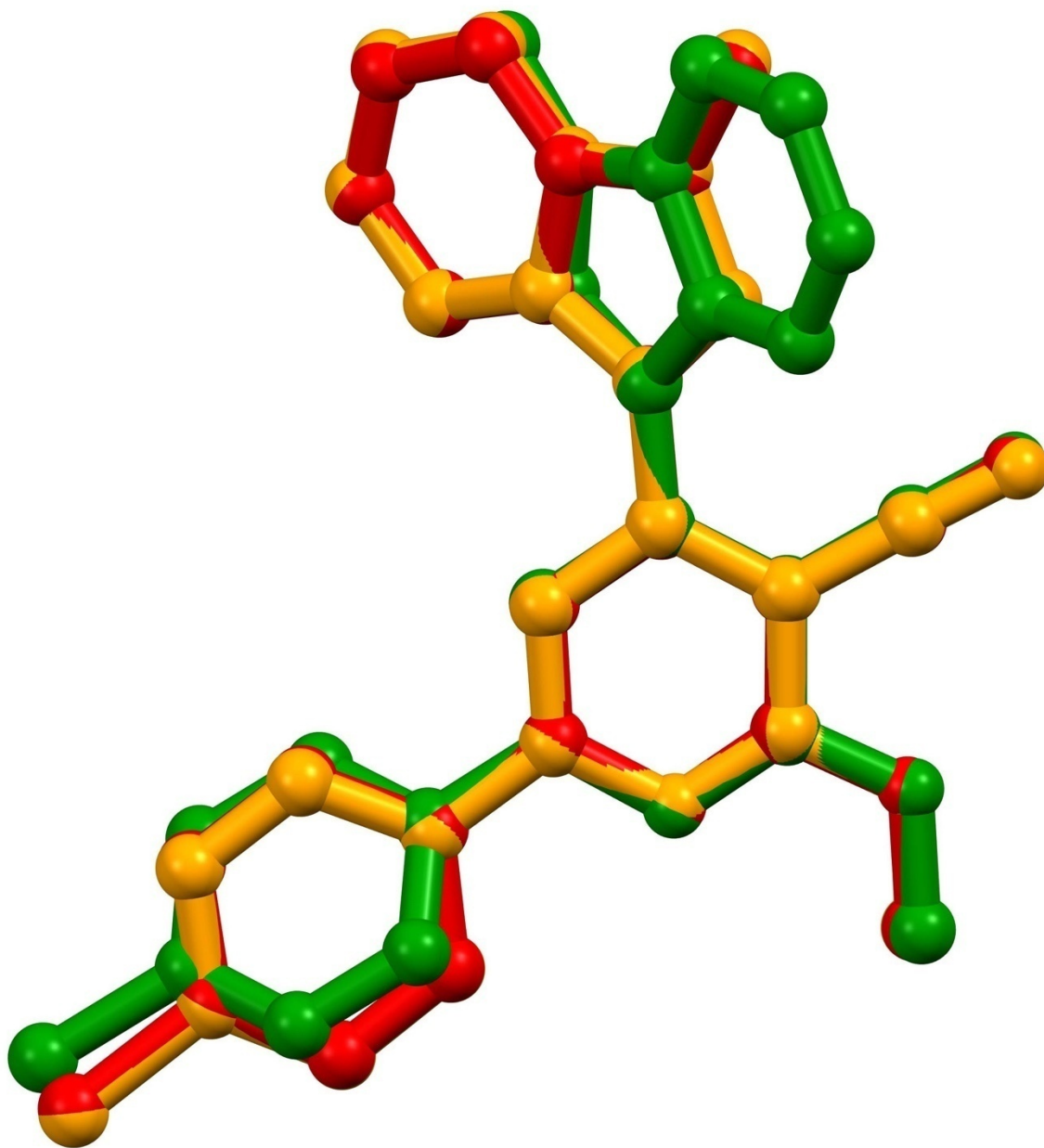


**Fig. S23.** Overlay view of compound **4b**, red (X-ray structure), green (free state DFT), yellow (DFT-d validation).



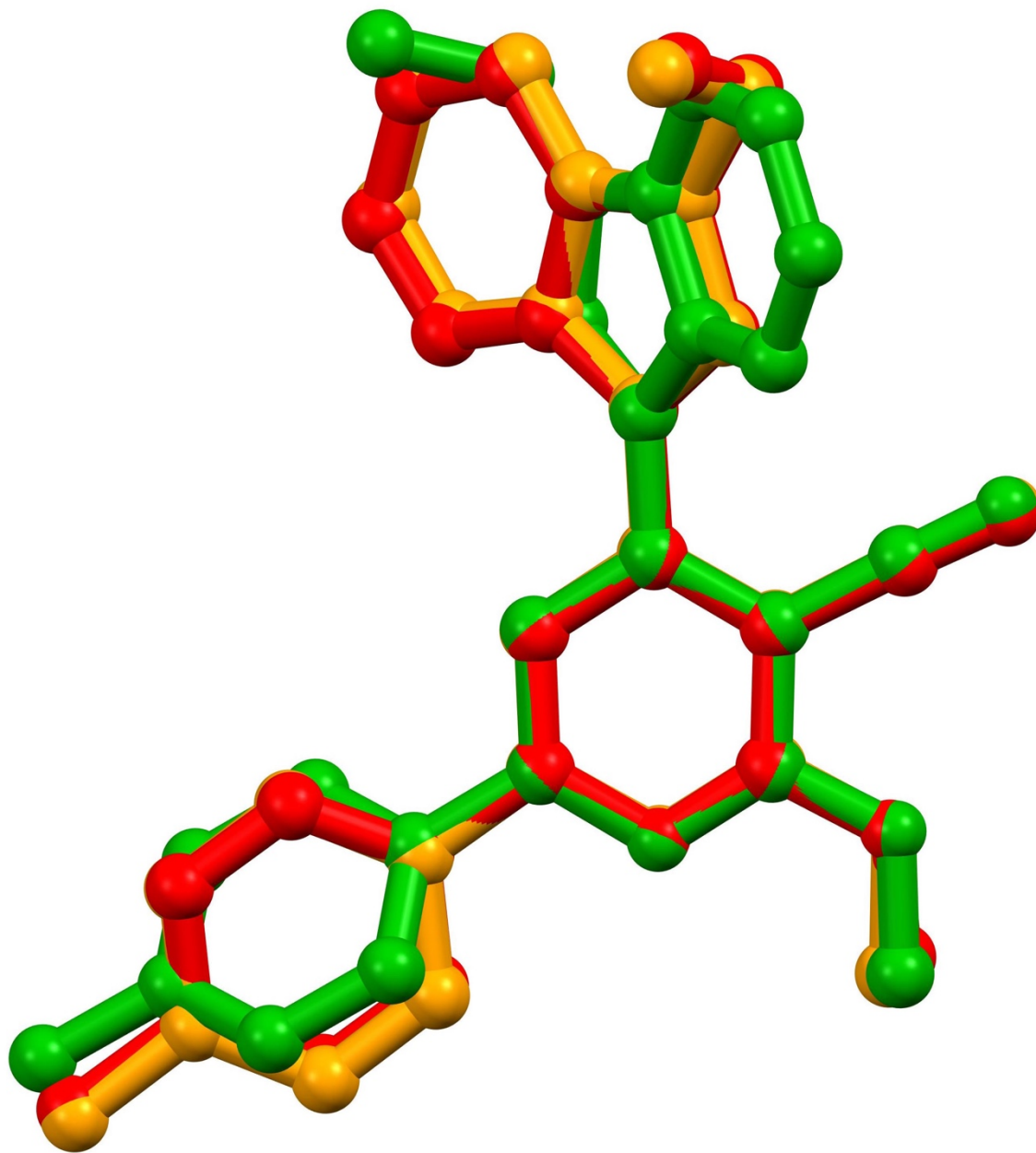


**Fig. S24.** Overlay view of compound **4c**, red (X-ray structure), green (free state DFT), yellow (DFT-d validation).

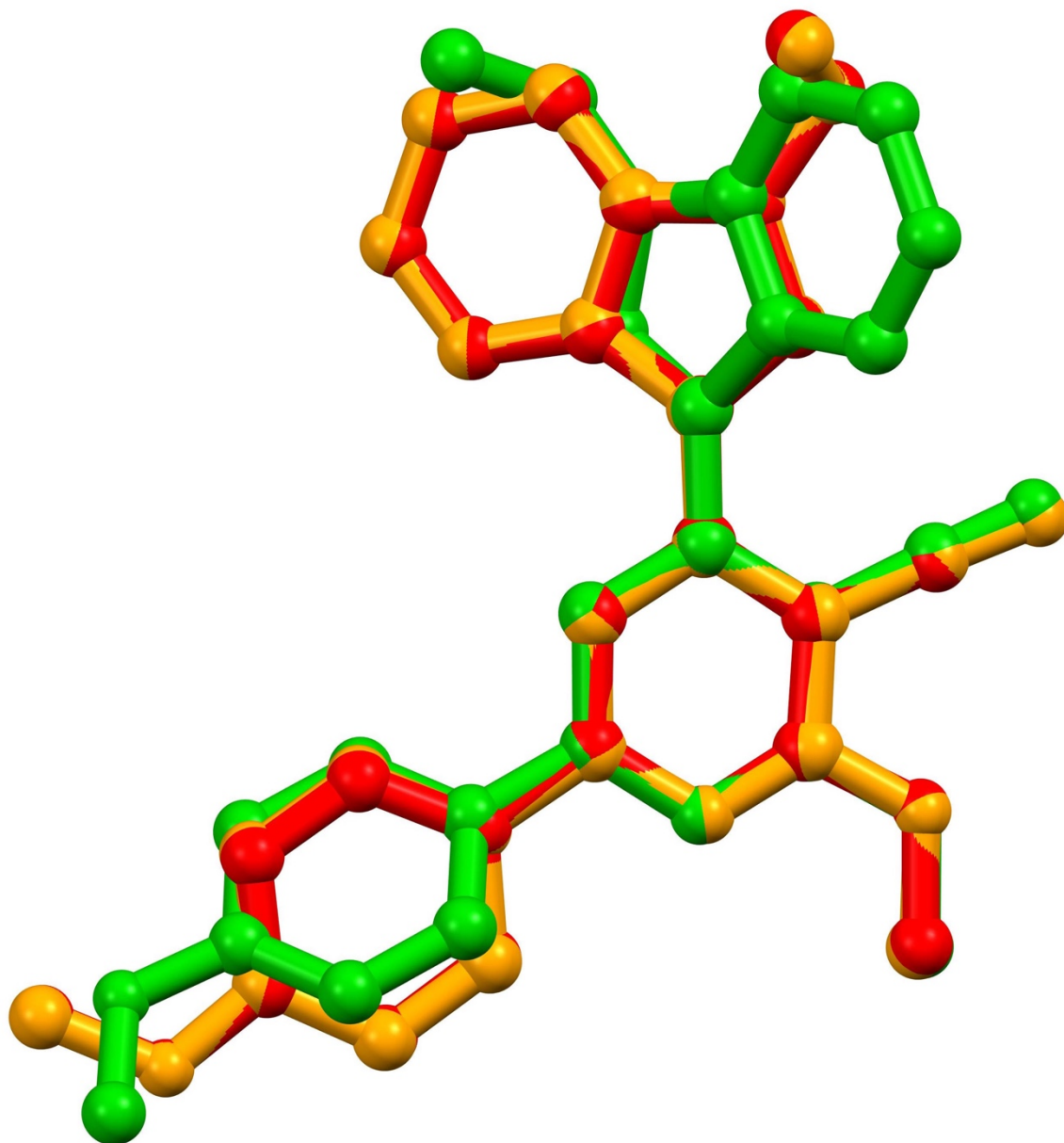


**Fig. S25.** Overlay view of compound **4d**, red (X-ray structure), green (free state DFT), yellow (DFT-d validation).

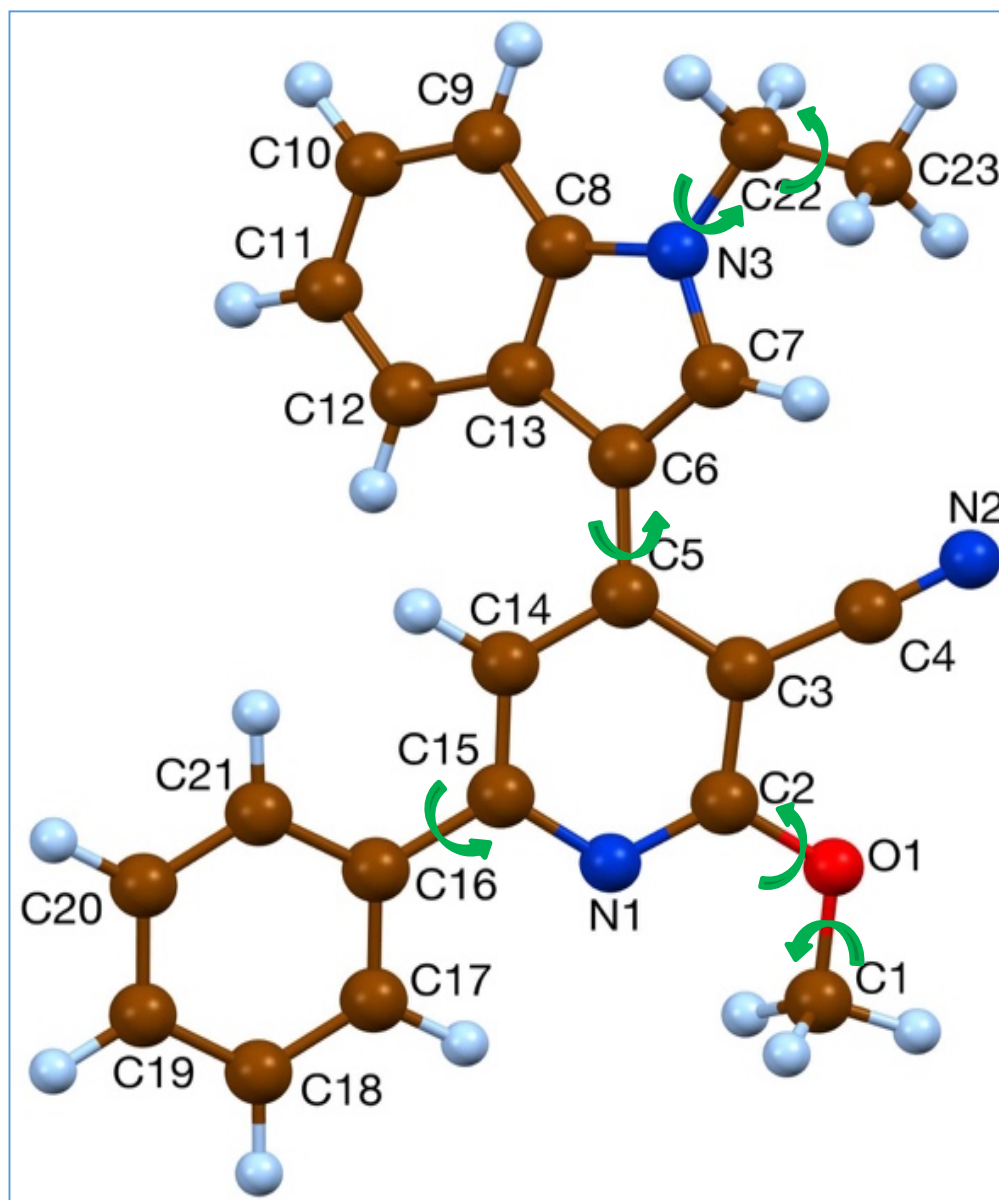


**Fig. S26.** The molecular structure of compound **4a** showing the atom-labeling scheme and the refined torsion angles (green arrows).

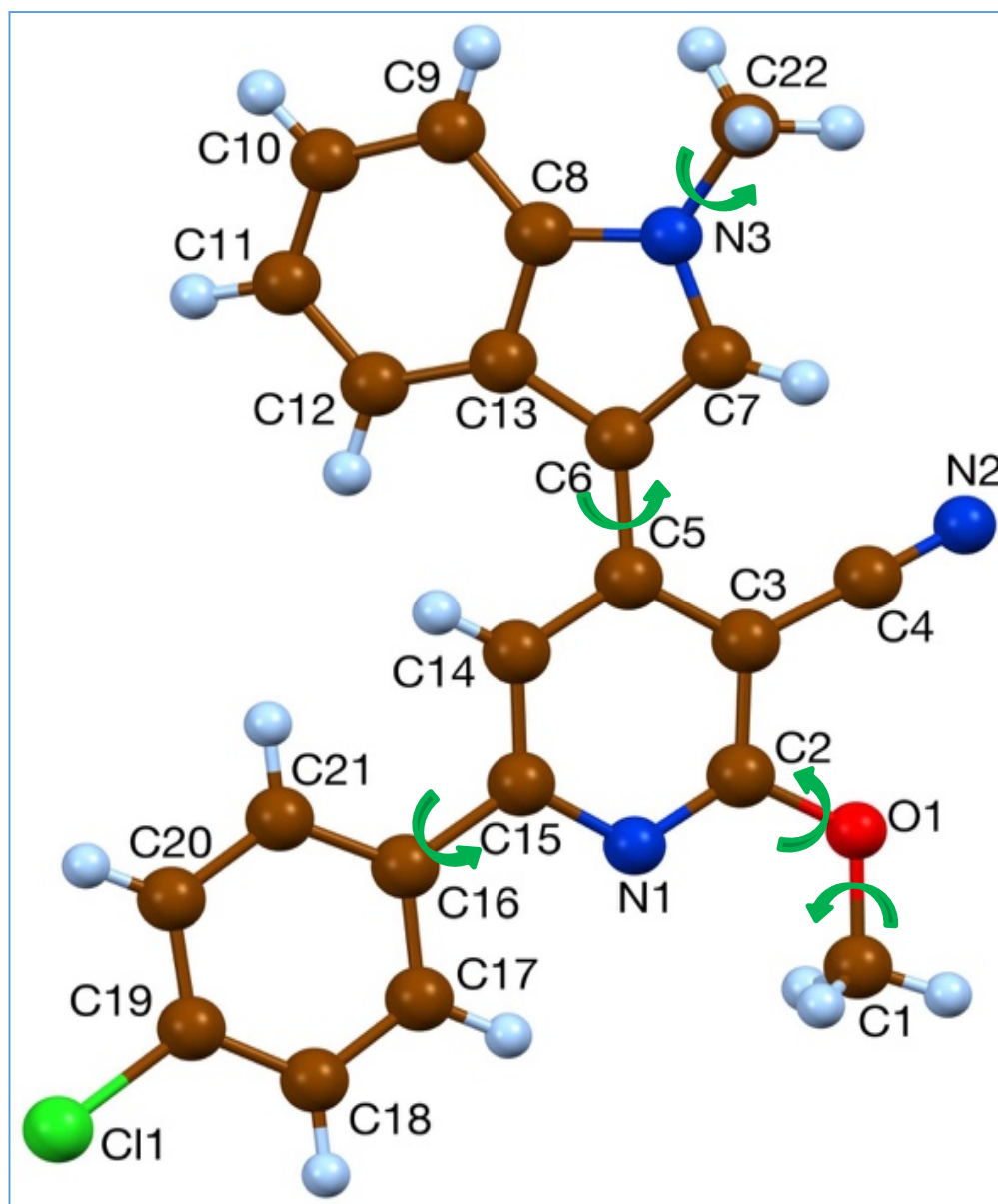


**Fig. S27.** The molecular structure of compound **4b** showing the atom-labeling scheme and the refined torsion angles (green arrows).

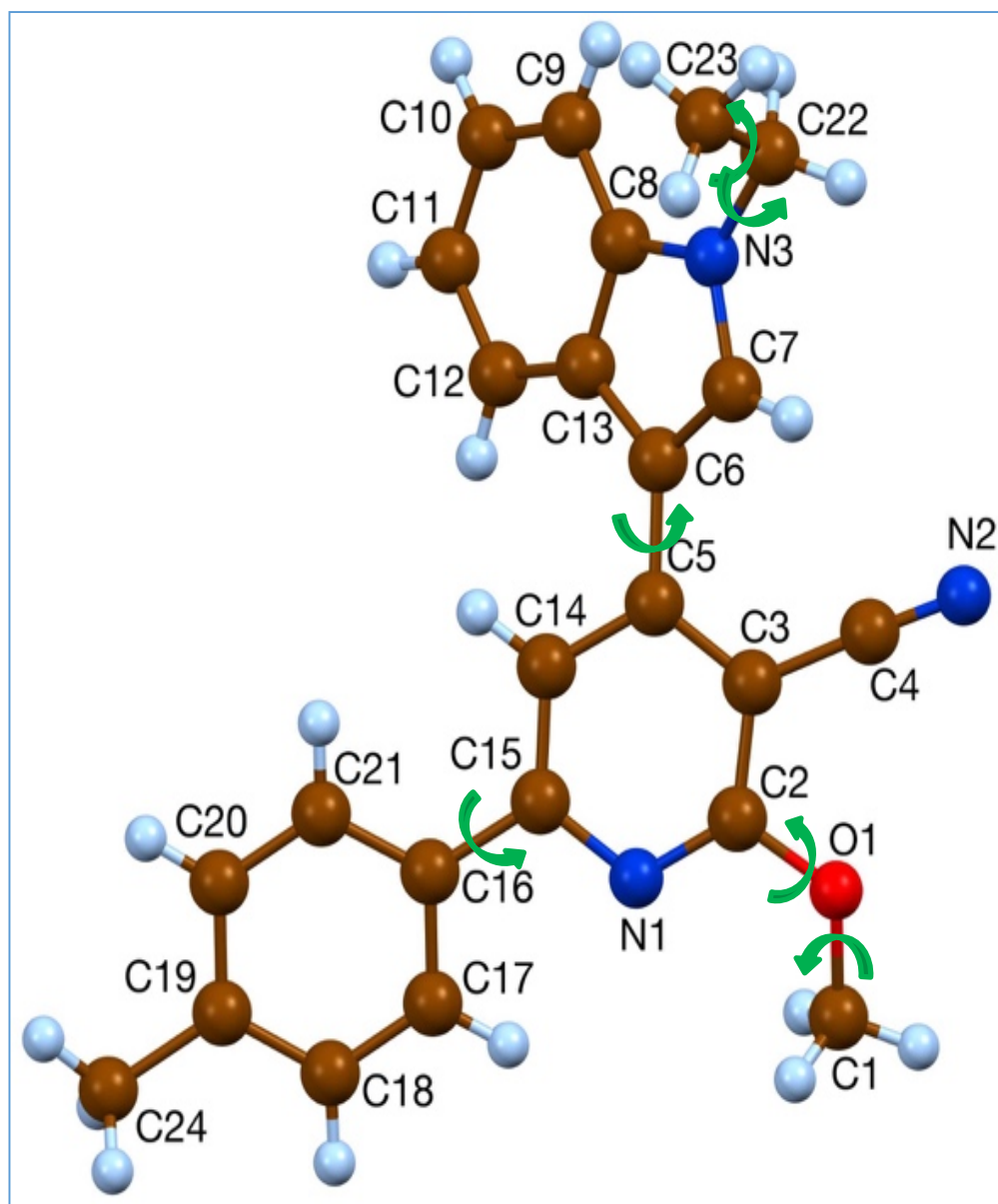


**Fig. S28.** The molecular structure of compound **4c** showing the atom-labeling scheme and the refined torsion angles (green arrows).

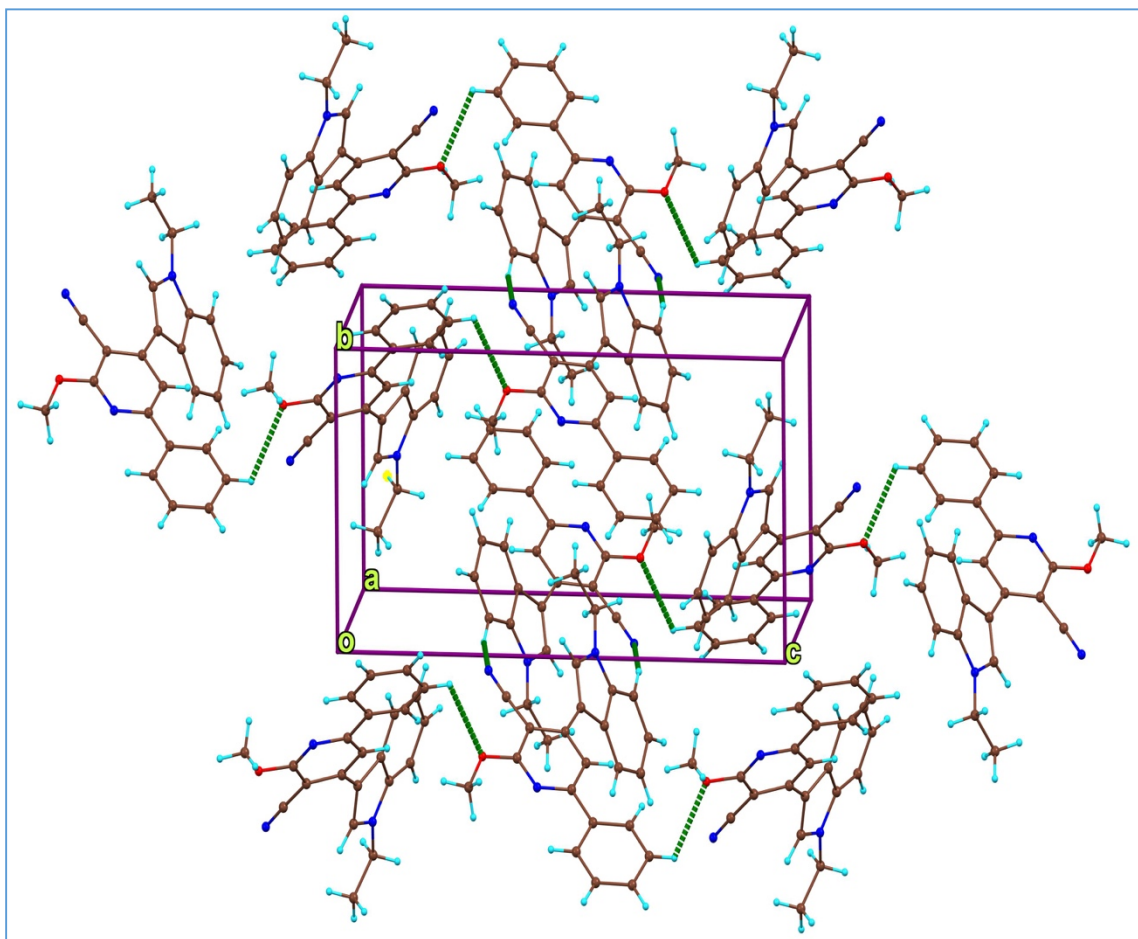


**Fig. S29.** Crystal packings in **4a**. Dashed lines denote intermolecular interactions.



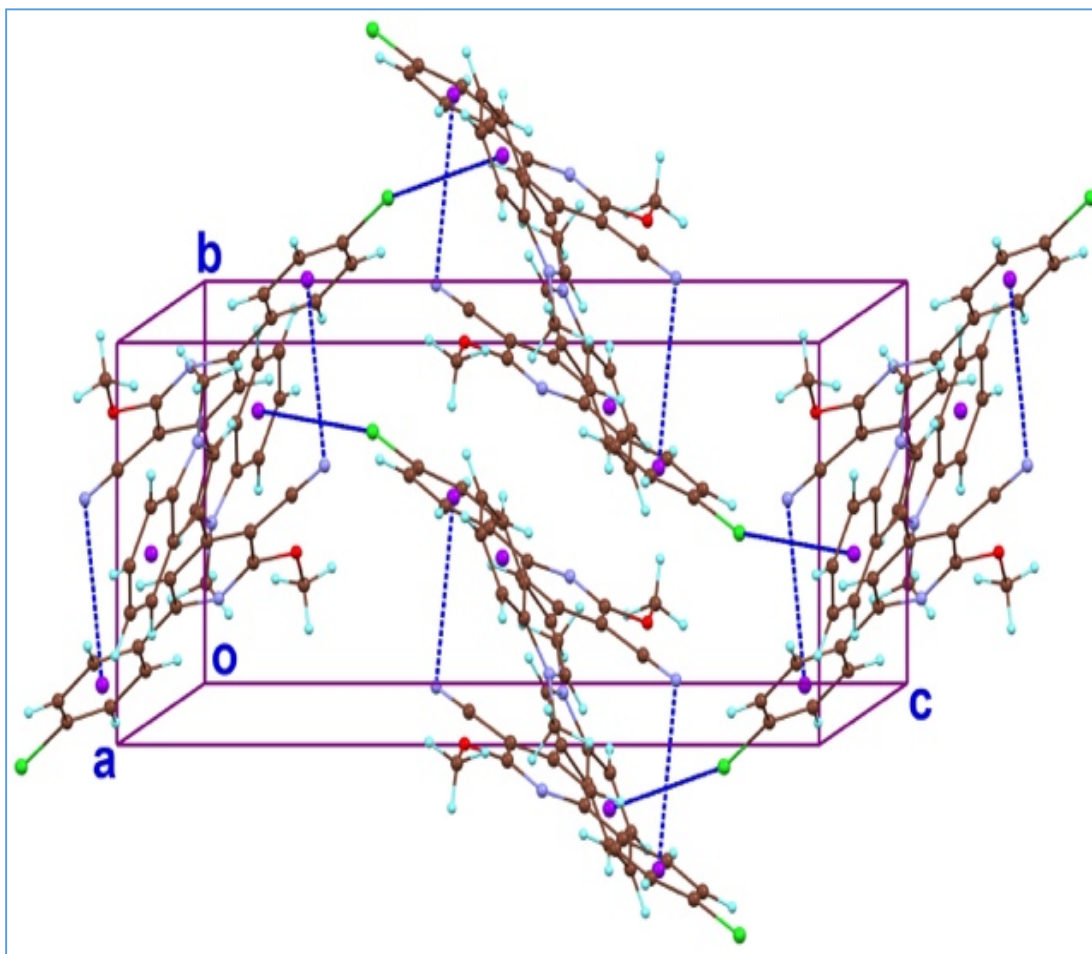


**Fig. S30.** Crystal packings in **4b**. Dashed lines denote intermolecular interactions.

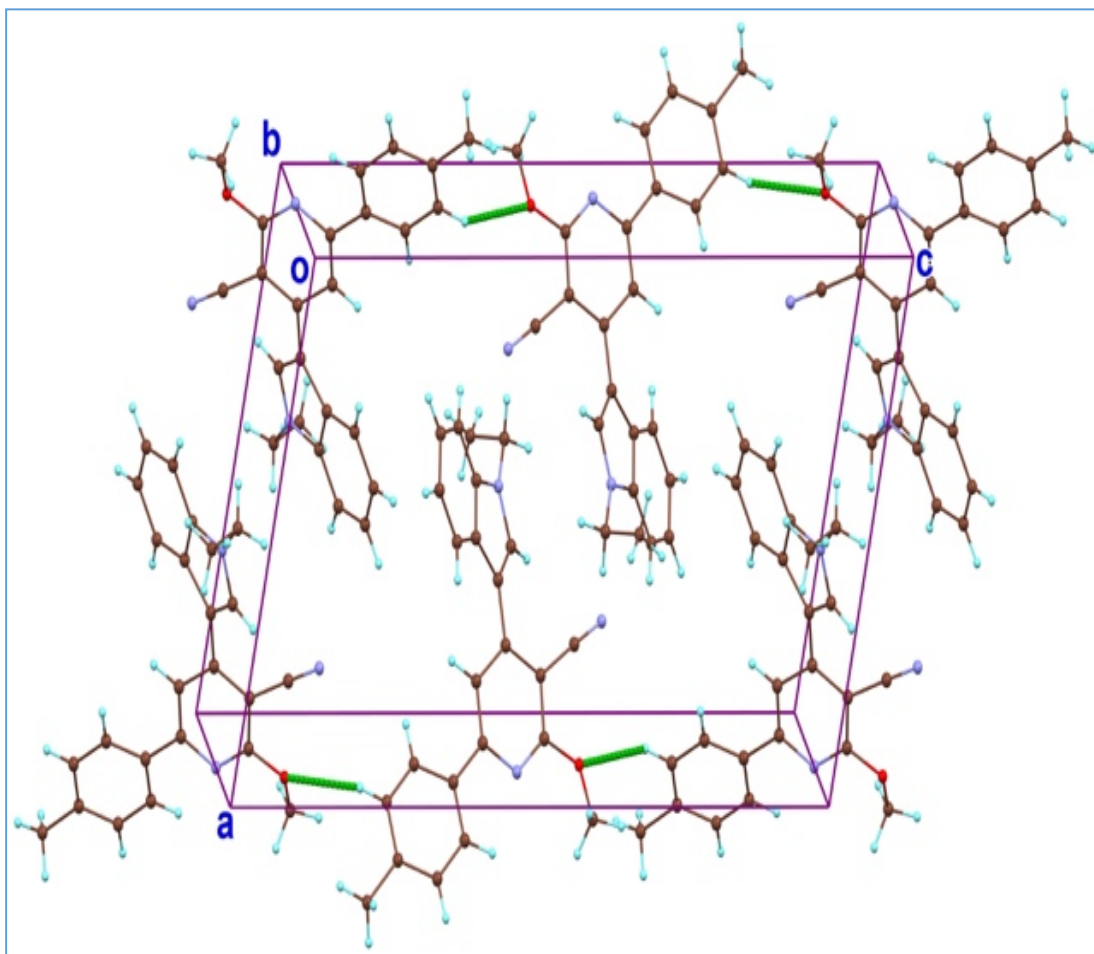


**Fig. S31.** Crystal packings in **4c**. Dashed lines denote intermolecular interactions.